Orbits Among Molecules. A Novel Way of Stereochemistry Through the Concepts of Coset Representations and Sphericities (Part 2)

Shinsaku Fujita

Department of Chemistry and Materials Technology,

Kyoto Institute of Technology,

Matsugasaki, Sakyoku, Kyoto 606-8585, Japan

E-mail: fujitas@chem.kit.ac.jp

Abstract

The present series is devoted to a diagrammatical introduction to the USCI (unit-subduced-cycle-index) approach developed by Fujita (S. Fujita, "Symmetry and Combinatorial Enumeration in Chemistry", Springer-Verlag, 1991). In Part 2 of this series, intermolecular stereochemistry (stereoisomerism) is discussed by the concept of *assembles of transformulas*. Transformulas that are generated from a skeleton of $\mathbf{G}$-symmetry having $|\mathbf{G}|$ vertices (i.e., a regular body representing the coset representation (CR) $\mathbf{G}(/\mathbf{C}_1)$) are equivalent under $\mathbf{G}$ so as to construct an orbit governed by the CR $\mathbf{G}(/\mathbf{C}_1)$. An assembly of $\mathbf{H}$-symmetry ($\mathbf{H} \subset \mathbf{G}$) is defined as a set of such transformulas as fixed by the action of $\mathbf{H}$. The set of equivalent $\mathbf{H}$-assemblies constructs an orbit of $\mathbf{H}$-assemblies, which is governed by the CR $\mathbf{G}(/\mathbf{H})$. Each $\mathbf{H}$-assembly corresponds to an $\mathbf{H}$-molecule derived from the skeleton of $\mathbf{G}$-symmetry. Thus the CR $\mathbf{G}(/\mathbf{H})$ is concluded to control the intermolecular stereochemistry (stereoisomerism). Thereby, subduction tables, USCI-CF tables (tables of unit-subduced-cycle-index with chirality fittingness), USCI tables (tables of unit-subduced-cycle-index without chirality fittingness), and mark tables for $\mathbf{D}_{2d}$ (as an example of $\mathbf{G}$) are obtained in

an alternative way to the method described in Part 1. The parallelism between Part 1 and Part 2 is clearly demonstrated by defining *a mandala* as a hypothetical structure (a nested regular body) in which the $|\mathbf{G}|$ transformulas generated as above from a regular body by the action of $\mathbf{G}$ are placed on the vertices of a regular body. Assembled mandalas and reduced mandalas are defined to integrate intermolecular and intramolecular stereochemistries.

1 Introduction

Stereochemistry has two fields, i.e., intramolecular stereochemistry and stereoisomerism (intermolecular stereochemistry), which should be studied in such an integrated manner as based on a common theoretical framework. In Part 1 of the series for a diagrammatical introduction of Fujita's USCI (unit-subduced-cycle-index) approach [1], the concept of *sphericity* has been shown to be a key concept for comprehending intramolecular stereochemistry. Before we show that the concept of sphericity works well in stereoisomerism (intermolecular stereochemistry), conventional approaches to stereoisomerism and to chemical combinatorics should be briefly discussed in order to show that they are deficient in such a common theoretical framework as the concept of sphericity.

1. Stereoisomerism (intermolecular stereochemistry) has been studied in terms of the permutational approach [2, 3, 4], where permutations of ligands have been considered to generate stereoisomers. These studies, however, have not taken the chirality/achirality of the ligands into explicit consideration. In other words, they have not taken account of inner structures in a molecule so that *they commonly lack the concept of sphericity* from the viewpoints of the present series of articles. For example, the concept of "a chemical identity group" proposed by Ugi et al. [4] is incapable of treating inner structures of a molecule (i.e., intramolecular stereochemistry), even though it works well in systematic discussions on stereoisomerism.[1] By an intimate examination of "the chemical identity group" and "the group of constitution preserving ligand permutation" in their treatment of the stereoisomers of trihydroxyglutaric acids (pages 146 to 150 of Ref. [4]), one can find that permutations of the same type are ascribed to enantiomeric relationships and diastereomeric relationships. The discrimination between enantiomers and diastereomers has been based on subsequent operations other than the permutations. The subsequent operations, which have been implicitly presumed to be reflections, have been treated subsidiarily as compared with the permutations.[2]

---

[1]This treatment is based on the presumption that substituents are selected from atoms (or achiral ligands). In other words, chiral ligands are not taken into explicit consideration.

[2]In terms of the permutation approach, the enantiomeric relationship between tetrahedral molecules (*R*-Cabcd and *S*-Cabcd) and the diastereomeric relationship between tetrahedral molecules (*r*-Cab$\ell^+\ell^-$ and *s*-Cab$\ell^+\ell^-$) are ascribed to the same permutation, where *R*-Cabcd (chiral), *S*-Cabcd (chiral), *r*-Cab$\ell^+\ell^-$ (achiral), and *s*-Cab$\ell^+\ell^-$ (achiral) are regarded as being in an equal level of consideration. Note that the symbols (a, b, c, and d) represent achiral ligands or atoms, while the symbols ℓ^+ and ℓ^- represent a pair of enantiomeric chiral ligands. The permutation of converting *R*-Cabcd (chiral) into *S*-Cabcd (chiral) coincides with a reflection operation, whereas the same permutation of converting *r*-Cab$\ell^+\ell^-$ (achiral) into *s*-Cab$\ell^+\ell^-$ (achiral) does not coincide with a reflection operation. This difference in the three-dimensional conversions has not been treated properly by the permutation approach. Obviously, the permutation approach has avoided such difficulties as described above by selecting only atoms (or achiral ligands) as substituents, so that it has unconsciously or consciously disregarded the cases of chiral ligands described above.

On the other hand, Fujita's USCI approach takes a balanced treatment in which a pair of *R*-Cabcd/*S*-Cabcd

2. Combinatorial enumeration of isomers depends on how (stereo)isomers are characterized symmetrically. Thus, the permutation approach for characterizing (stereo)isomers has been implicitly involved in Pólya's theorem [5, 6], which has been widely used in chemical combinatorics [7]. As found in his famous article [5, 6], the term *configurations* has been used to refer to isomers generated by permutations. Such isomers as enumerated by Pólya's theorem have been found to be graphs, not three-dimensional (3D) chemical structures. This means that *Pólya's theorem also lacks the concept of sphericity*, as pointed out in recent articles [8, 9].

3. Because Pólya's theorem is based on "conjugacy classes" (as equivalent classes with respect to "conjugacy of elements") but not on "orbits" (as equivalence classes with respect to "conjugate subgroups"),[3] the viewpoint to formulate "configurations" is limited within the scope of "conjugacy classes". It follows that Pólya's theorem *does* enumerate graphs without symmetry-itemization, as discussed in Chapter 13 of Fujita's book [10]. On the other hand, Fujita's USCI approach has provided another viewpoint to formulate "configurations" on the basis of the concept of CRs (and sphericities), as discussed in Chapter 15 of Fujita's book [10]. Thereby, Fujita's USCI approach can enumerate stereoisomers (3D chemical structures) with symmetry-itemization. Note that "stereoisomers" are more informative than "graphs" and that "accomplishing symmetry-itemization" is more informative than "no symmetry-itemization". Thus, Fujita's USCI approach can derive Pólya's theorem [11] but the reverse is impossible without additional information. More detailed aspects have been pointed out in a recent article [12].

In addition to the original mathematical treatment [10], Fujita's USCI approach to stereoisomerism (intermolecular stereochemistry) has been visualized in terms of "graphical models" [13, 14, 15]. This visualization, however, has not explicitly involved the concept of sphericity. It follows that the visualization has not directly aimed at chemical combinatorics that is one of the most important disciplines accomplished by Fujita's USCI approach.

The present paper (Part 2) will demonstrate diagrammatically that the concept of *sphericity* works also in stereoisomerism (intermolecular stereochemistry). This diagrammatical demonstration will be further reinforced by the concept of *mandala*, which will be proposed to give a more sophisticated approach for characterizing sphericities in stereoisomerism. As a result, the sphericity will be shown to control intra- and intermolecular stereochemistries concurrently, so that it will provide prerequisites for chemical combinatorics (Part 3).
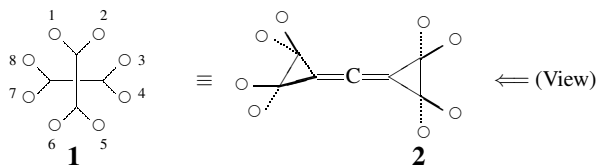
2 Stereoisomerism

Let us adopt the same topview (**1**) of the regular body as adopted in Part 1. The regular body (**1**) belongs to the point group $\mathbf{D}_{2d}$, as shown in Fig. 1. In this section, the viewpoint of the

---

(totally achiral), r-Cab$\ell^+\ell^-$ (achiral), and s-Cab$\ell^+\ell^-$ (achiral) are considered to be in an equal level of consideration. Furthermore, the pair of R-Cabcd/S-Cabcd (totally achiral) is characterized by the enantiosphericity in stereoisomerism, while the achiral molecule r-Cab$\ell^+\ell^-$ (or s-Cab$\ell^+\ell^-$) is characterized by the homosphericity in stereoisomerism. These further points are the subjects of Part 2.

[3]This feature is analogous to a chemical feature that, although the concept of "atoms" is essential to chemistry, an additional concept of "molecules" is necessary to comprehend chemical phenomena. In analogy, although the concept of "conjugacy classes" is essential to group theory, an additional concept "conjugate subgroups" is necessary to comprehend symmetrical phenomena.

Figure 1: Regular body for $\mathbf{D}_{2d}$.

USCI approach is restated in order to show that the concept of sphericity works well to discuss stereoisomerism as well as intramolecular stereochemistry.

2.1 Assemblies of Transformulas and Orbits of Assemblies

2.1.1 C_1-Assembly as an Extreme Case

Let us select the regular body **1** as a *reference transformula*,[4] the numbering of which is regarded as a reference numbering.[5] As shown in Part I, the action of the symmetry operations of $\mathbf{D}_{2d}$ on **1** as a reference transformula gives other transformulas (e.g., **3**). Thus, the eight transformulas shown in Fig. 2 are obtained on the action of every symmetry operations so that they are considered to construct a set of transformulas: $\mathcal{T} = \{\mathbf{1}, \mathbf{3}, \mathbf{4}, \mathbf{5}, \mathbf{6}, \mathbf{7}, \mathbf{8}, \mathbf{9}\}$. To relate intramolecular stereochemistry (Part 1) to stereoisomerism,[6] the ordered set is numbered as follows:

$$\mathcal{T}_\alpha = \{f_1, f_5, f_4, f_8, f_2, f_6, f_7, f_3\}. \tag{1}$$

The action of a symmetry operation $C_{2(3)}$ on the every transformulas listed in Fig. 2 generates another ordered set of the transformulas, i.e., $\mathcal{T}_\beta = \{\mathbf{3}, \mathbf{1}, \mathbf{5}, \mathbf{4}, \mathbf{7}, \mathbf{6}, \mathbf{9}, \mathbf{8}\}$, as shown in Fig. 3. This corresponds to the ordered set: $\mathcal{T}_\beta = \{f_5, f_1, f_8, f_4, f_6, f_2, f_7, f_3\}$. The conversion $\mathcal{T}_\alpha \rightarrow \mathcal{T}_\beta$ generates the following permutation:

$$C_{2(3)} \sim \begin{pmatrix} f_1 & f_5 & f_4 & f_8 & f_2 & f_6 & f_7 & f_3 \\ f_5 & f_1 & f_8 & f_4 & f_6 & f_2 & f_3 & f_7 \end{pmatrix}$$

$$\sim \begin{pmatrix} 1 & 2 & 3 & 4 & 5 & 6 & 7 & 8 \\ 5 & 6 & 7 & 8 & 1 & 2 & 3 & 4 \end{pmatrix} = (1\,5)(2\,6)(3\,7)(4\,8), \tag{2}$$

where the first permutation is reordered sequentially with respect to the upper row and the subscript of each transformula is adopted to generate the second permutation. Because the group $\mathbf{D}_{2d}$ has eight symmetry operations, such diagrammatical expressions as Figs. 2 and 3 can be obtained for every symmetry operations of $\mathbf{D}_{2d}$ (e.g., Fig. 2 for I and Fig. 3 for $C_{2(3)}$).

---

[4]For the coinage of the term *transformula*, see Part 1. A reference transformula is defined as a numbered skeleton substituted by objects (atoms, ligands, etc.), where the numbered skeleton belongs to the point group **G**. The reference transformula is transformed into other transformulas on the action of **G**.

[5]There are 8! modes of numbering, among which the reference numbering adopted here generates only 8 modes of numbering because the $\mathbf{D}_{2d}$-symmetry is chosen. If another numbering is adopted as a reference, another set of 8 modes of numbering can be generated. These two selections give equivalent results through conjugate relationships within the symmetric group of degree 8.

[6]The alignment of $\mathcal{T}_\alpha$ is so selected as to give the same permutations as derived from $\mathcal{R} = \{1, 2, 3, 4, 5, 6, 7, 8\}$. Although other modes of numbering give other permutations, these are equivalent to the present one without considering the modes of numbering.
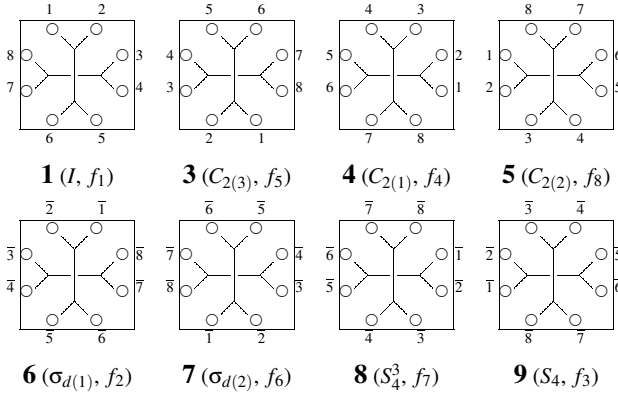
Figure 2: Eight $\mathbf{C}_1$-assemblies, each of which contains either one of eight transformulas (f_1–f_8). The assembly represents a single molecule. The alignment shown in this diagram corresponds to an ordered set, $\mathcal{T}_\alpha = \{f_1, f_5, f_4, f_8, f_2, f_6, f_7, f_3\}$, which is an orbit governed by the regular representation $\mathbf{D}_{2d}(/\mathbf{C}_1)$.
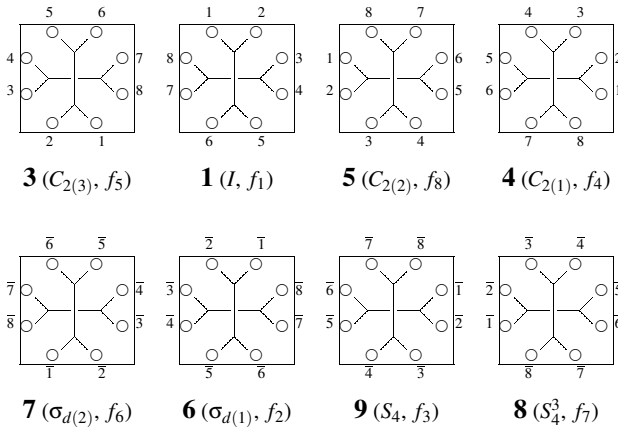

Figure 3: The action of $C_{2(3)}$ on the orbit of the eight $\mathbf{C}_1$-assemblies shown in Fig. 2, producing another ordered set: $\mathcal{T}_\beta = \{f_5, f_1, f_8, f_4, f_6, f_2, f_3, f_7\}$. The orbit of transformulas is governed by the regular representation $\mathbf{D}_{2d}(/\mathbf{C}_1)$.

Thereby, eight permutations can be obtained in a similar procedure for obtaining eq. 2 as follows:

$$I \sim \begin{pmatrix} f_1 & f_2 & f_3 & f_4 & f_5 & f_6 & f_7 & f_8 \\ f_1 & f_2 & f_3 & f_4 & f_5 & f_6 & f_7 & f_8 \end{pmatrix} \sim (1)(2)(3)(4)(5)(6)(7)(8) \tag{3}$$

$$C_{2(3)} \sim \begin{pmatrix} f_1 & f_2 & f_3 & f_4 & f_5 & f_6 & f_7 & f_8 \\ f_5 & f_6 & f_7 & f_8 & f_1 & f_2 & f_3 & f_4 \end{pmatrix} \sim (1\,5)(2\,6)(3\,7)(4\,8) \tag{4}$$

$$C_{2(1)} \sim \begin{pmatrix} f_1 & f_2 & f_3 & f_4 & f_5 & f_6 & f_7 & f_8 \\ f_4 & f_3 & f_2 & f_1 & f_8 & f_7 & f_6 & f_5 \end{pmatrix} \sim (1\,4)(2\,3)(5\,8)(6\,7) \tag{5}$$

$$C_{2(2)} \sim \begin{pmatrix} f_1 & f_2 & f_3 & f_4 & f_5 & f_6 & f_7 & f_8 \\ f_8 & f_7 & f_6 & f_5 & f_4 & f_3 & f_2 & f_1 \end{pmatrix} \sim (1\,8)(2\,7)(3\,6)(4\,5) \tag{6}$$

$$\sigma_{d(1)} \sim \begin{pmatrix} f_1 & f_2 & f_3 & f_4 & f_5 & f_6 & f_7 & f_8 \\ f_2 & f_1 & f_8 & f_7 & f_6 & f_5 & f_4 & f_3 \end{pmatrix} \sim \overline{(1\,2)(3\,8)(4\,7)(5\,6)} \tag{7}$$

$$\sigma_{d(2)} \sim \begin{pmatrix} f_1 & f_2 & f_3 & f_4 & f_5 & f_6 & f_7 & f_8 \\ f_6 & f_5 & f_4 & f_3 & f_2 & f_1 & f_8 & f_7 \end{pmatrix} \sim \overline{(1\,6)(2\,5)(3\,4)(7\,8)} \tag{8}$$

$$S_4^3 \sim \begin{pmatrix} f_1 & f_2 & f_3 & f_4 & f_5 & f_6 & f_7 & f_8 \\ f_3 & f_8 & f_5 & f_2 & f_7 & f_4 & f_1 & f_6 \end{pmatrix} \sim \overline{(1\,3\,5\,7)(2\,8\,6\,4)} \tag{9}$$

$$S_4 \sim \begin{pmatrix} f_1 & f_2 & f_3 & f_4 & f_5 & f_6 & f_7 & f_8 \\ f_7 & f_4 & f_1 & f_6 & f_3 & f_8 & f_5 & f_2 \end{pmatrix} \sim \overline{(1\,7\,5\,3)(2\,4\,6\,8)} \tag{10}$$

where each overbar represents the mirror image of each object. They are equivalent to the permutations shown in eqs. 14–21 of Part 1.[7] These permutations construct a permutation representation that is equalized to be a CR $\mathbf{D}_{2d}(/\mathbf{C}_1)$.

The above-described procedure implies that, although the eight transformulas are regarded as being different from one another by considering the modes of numbering, they are equivalent on the action of $\mathbf{D}_{2d}$. Strictly speaking, each of the eight transformulas is considered to be *a* $\mathbf{C}_1$-*assembly* (as a one-membered assembly), which is produced by the subduction $\mathbf{D}_{2d}(/\mathbf{C}_1) \downarrow \mathbf{C}_1 = 8\mathbf{C}_1(/\mathbf{C}_1)$.[8] Note that the eight $\mathbf{C}_1$-assemblies (one-membered assemblies) shown in Fig. 2 construct an orbit, which is governed by $\mathbf{D}_{2d}(/\mathbf{C}_1)$. This fact is emphasized by adding a box surrounding each of the transformulas in Figs. 2 and 3. As a result, **1** is fixed only by $\mathbf{C}_1$ so as to belong to $\mathbf{C}_1$, which appears as the local symmetry of the CR $\mathbf{D}_{2d}(/\mathbf{C}_1)$.

2.1.2 $\mathbf{C}_s$-Assemblies and Their Orbit

Let us consider transformulas generated from a regular body of $\mathbf{G}$-symmetry. An assembly of transformulas is defined as a set of transformulas that produces equivalent sets of transformulas on the action of $\mathbf{G}$, where any two of such sets can be so selected as to have no common transformulas. The term *assemblies of transformulas* can be regarded as an analogy to the term "segments of objects" in a regular body. If such assemblies have a chemical meaning, they are called *molecules* on the analogy to the description that segments having chemical meanings are called *ligands* (cf. Part 1). As an extreme case, this feature has been described above for the case of $\mathbf{C}_1$-assemblies. The present subsection deals with more general cases of assemblies.

---

[7]Strictly speaking, this representation corresponds to left cosets $g^{-1}\mathbf{C}_1$ ($g \in \mathbf{D}_{2d}$), while eqs. 14–21 of Part 1 corresponds to right cosets $\mathbf{C}_1 g$.

[8]For a new-defined meaning of the word "assembly", see Part 1. This is an extreme case of an assemblage pattern described below.

Let us consider an assembly represented by $\mathcal{A}_1^* = \{f_1, f_2\}$ (i.e., $\{\mathbf{1}, \mathbf{6}\}$), as surrounded by a box in Fig. 4. By applying symmetry operations of $\mathbf{D}_{2d}$ onto $\mathcal{A}_1^*$, other assemblies ($\mathcal{A}_2^* = \{f_4, f_7\}$, $\mathcal{A}_3^* = \{f_5, f_6\}$, and $\mathcal{A}_4^* = \{f_8, f_3\}$) are obtained diagrammatically. Then, they are gathered to give a set of assemblies, which is considered to be an ordered set:

$$\mathcal{A}^* = \{\mathcal{A}_1^*, \mathcal{A}_3^*, \mathcal{A}_2^*, \mathcal{A}_4^*\}, \tag{11}$$

where the concrete assemblies are depicted in Fig. 4. Obviously, the four assemblies involved in the right-hand side of eq. 11 are equivalent on the action of $\mathbf{D}_{2d}$, constructing an orbit. Because the assembly $\mathcal{A}_1^*$ is fixed on the action of $\mathbf{C}_s$ (i.e., f_1 and f_2 are equivalent under $\mathbf{C}_s$), the local symmetry of $\mathcal{A}_1^*$ is determined to be $\mathbf{C}_s$. It follows that the orbit $\mathcal{A}^*$ (eq. 11) is governed by the CR $\mathbf{D}_{2d}(/\mathbf{C}_s)$.

The action of a symmetry operation $C_{2(3)}$ on every transformulas of Fig. 4 (corresponding to the ordered set represented by eq. 11) gives transformulas shown in Fig. 5 (corresponding to the ordered set, i.e., $\mathcal{A}_\alpha^* = \{\mathcal{A}_1^*, \mathcal{A}_2^*, \mathcal{A}_3^*, \mathcal{A}_4^*\}$). This process is expressed by the following permutation:

$$\begin{pmatrix} \mathcal{A}_1^* & \mathcal{A}_3^* & \mathcal{A}_2^* & \mathcal{A}_4^* \\ \mathcal{A}_3^* & \mathcal{A}_1^* & \mathcal{A}_4^* & \mathcal{A}_2^* \end{pmatrix} = \begin{pmatrix} \mathcal{A}_1^* & \mathcal{A}_2^* & \mathcal{A}_3^* & \mathcal{A}_4^* \\ \mathcal{A}_3^* & \mathcal{A}_4^* & \mathcal{A}_1^* & \mathcal{A}_2^* \end{pmatrix}$$
$$\sim \begin{pmatrix} 1 & 2 & 3 & 4 \\ 3 & 4 & 1 & 2 \end{pmatrix} = (1\,3)(2\,4). \tag{12}$$

The permutation is essentially equal to that of eq. 22 of Part 1, when reordered as above with respect to the top row. Similarly, we can obtain the following permutations (as products of cycles) for the respective operations:

$$I \sim \begin{pmatrix} \mathcal{A}_1^* & \mathcal{A}_2^* & \mathcal{A}_3^* & \mathcal{A}_4^* \\ \mathcal{A}_1^* & \mathcal{A}_2^* & \mathcal{A}_3^* & \mathcal{A}_4^* \end{pmatrix} \sim (1)(2)(3)(4) \tag{13}$$

$$C_{2(3)} \sim \begin{pmatrix} \mathcal{A}_1^* & \mathcal{A}_2^* & \mathcal{A}_3^* & \mathcal{A}_4^* \\ \mathcal{A}_3^* & \mathcal{A}_4^* & \mathcal{A}_1^* & \mathcal{A}_2^* \end{pmatrix} \sim (1\,3)(2\,4) \tag{14}$$

$$C_{2(1)} \sim \begin{pmatrix} \mathcal{A}_1^* & \mathcal{A}_2^* & \mathcal{A}_3^* & \mathcal{A}_4^* \\ \mathcal{A}_2^* & \mathcal{A}_1^* & \mathcal{A}_4^* & \mathcal{A}_3^* \end{pmatrix} \sim (1\,2)(3\,4) \tag{15}$$

$$C_{2(2)} \sim \begin{pmatrix} \mathcal{A}_1^* & \mathcal{A}_2^* & \mathcal{A}_3^* & \mathcal{A}_4^* \\ \mathcal{A}_4^* & \mathcal{A}_3^* & \mathcal{A}_2^* & \mathcal{A}_1^* \end{pmatrix} \sim (1\,4)(2\,3) \tag{16}$$

$$\sigma_{d(1)} \sim \begin{pmatrix} \mathcal{A}_1^* & \mathcal{A}_2^* & \mathcal{A}_3^* & \mathcal{A}_4^* \\ \overline{\mathcal{A}}^*_1 & \overline{\mathcal{A}}^*_4 & \overline{\mathcal{A}}^*_3 & \overline{\mathcal{A}}^*_2 \end{pmatrix} \sim \overline{(1)(2\,4)(3)} \tag{17}$$

$$\sigma_{d(2)} \sim \begin{pmatrix} \mathcal{A}_1^* & \mathcal{A}_2^* & \mathcal{A}_3^* & \mathcal{A}_4^* \\ \overline{\mathcal{A}}^*_3 & \overline{\mathcal{A}}^*_2 & \overline{\mathcal{A}}^*_1 & \overline{\mathcal{A}}^*_4 \end{pmatrix} \sim \overline{(1\,3)(2)(4)} \tag{18}$$

$$S_4^3 \sim \begin{pmatrix} \mathcal{A}_1^* & \mathcal{A}_2^* & \mathcal{A}_3^* & \mathcal{A}_4^* \\ \overline{\mathcal{A}}^*_4 & \overline{\mathcal{A}}^*_1 & \overline{\mathcal{A}}^*_2 & \overline{\mathcal{A}}^*_3 \end{pmatrix} \sim \overline{(1\,4\,3\,2)} \tag{19}$$

$$S_4 \sim \begin{pmatrix} \mathcal{A}_1^* & \mathcal{A}_2^* & \mathcal{A}_3^* & \mathcal{A}_4^* \\ \overline{\mathcal{A}}^*_2 & \overline{\mathcal{A}}^*_3 & \overline{\mathcal{A}}^*_4 & \overline{\mathcal{A}}^*_1 \end{pmatrix} \sim \overline{(1\,2\,3\,4)} \tag{20}$$

It follows that eqs. 13—20 represent a concrete form of the CR $\mathbf{D}_{2d}(/\mathbf{C}_s)$, which governs the orbit of the assemblies, i.e., $\mathcal{A}^* = \{\mathcal{A}_1^*, \mathcal{A}_2^*, \mathcal{A}_3^*, \mathcal{A}_4^*\}$. The set of the permutations (eqs. 13—20) is essentially the same as the set of the permutations (eqs. 23–30 of Part 1) for the set
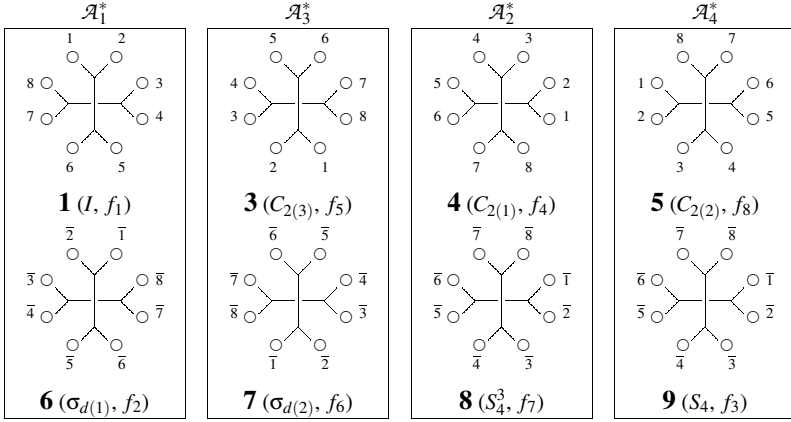
Figure 4: Assemblies for representing the CR $\mathbf{D}_{2d}(/\mathbf{C}_s)$. The four assemblies, $\mathcal{A}_1^* = \{f_1, f_2\}$ $\mathcal{A}_2^* = \{f_4, f_7\}$, $\mathcal{A}_3^* = \{f_5, f_6\}$, and $\mathcal{A}_4^* = \{f_8, f_3\}$, construct an ordered set of assemblies, i.e., $\mathcal{A}_\alpha^* = \{\mathcal{A}_1^*, \mathcal{A}_3^*, \mathcal{A}_2^*, \mathcal{A}_4^*\}$, which is an orbit governed by the CR $\mathbf{D}_{2d}(/\mathbf{C}_s)$.
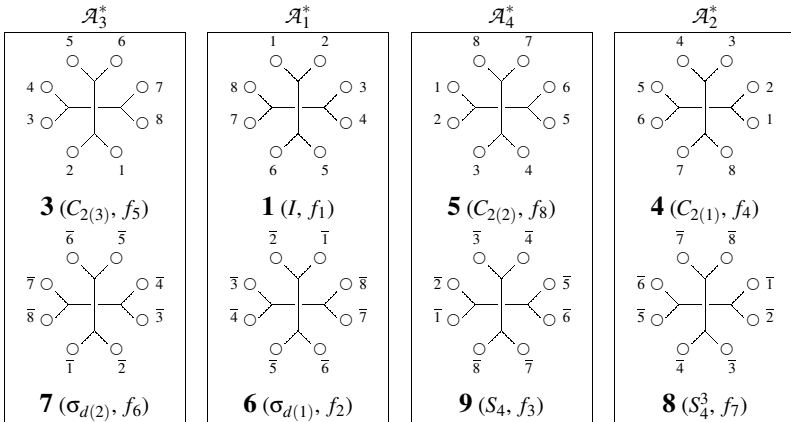

Figure 5: The action of $C_{2(3)}$ on the orbit of assemblies shown in Fig. 4, producing another ordered set, i.e., $\mathcal{A}_\beta^* = \{\mathcal{A}_3^*, \mathcal{A}_1^*, \mathcal{A}_4^*, \mathcal{A}_2^*\}$, where the four assemblies represented by $\mathcal{A}_1^* = \{f_1, f_2\}$ $\mathcal{A}_2^* = \{f_4, f_7\}$, $\mathcal{A}_3^* = \{f_5, f_6\}$, and $\mathcal{A}_4^* = \{f_8, f_3\}$. The orbit of assemblies is governed by the CR $\mathbf{D}_{2d}(/\mathbf{C}_s)$.

of segments $\mathcal{A} = \{\mathcal{A}_1, \mathcal{A}_2, \mathcal{A}_3, \mathcal{A}_4\}$.[9] This fact reflects the parallelism between intramolecular stereochemistry and stereoisomerism.

Exercise 1. Derive eqs. 13–20 by drawing such figures as Fig. 4 (eq. 13 for I) and Fig. 5 (eq. 14 for $C_{2(3)}$).

It is worthwhile to add some commentaries to the procedure above from the viewpoint of group theory. The symmetry operations listed in Fig. 4 are categorized into cosets derived from the coset decomposition of $\mathbf{D}_{2d}$ by the subgroup $\mathbf{C}_s$ as follows:

$$\mathbf{D}_{2d} = I\mathbf{C}_s + C_{2(3)}\mathbf{C}_s + C_{2(1)}\mathbf{C}_s + C_{2(2)}\mathbf{C}_s \tag{21}$$

$$= \underbrace{\{I, \sigma_{d(1)}\}}_{\mathcal{A}_1^*} + \underbrace{\{C_{2(3)}, \sigma_{d(2)}\}}_{\mathcal{A}_3^*} + \underbrace{\{C_{2(1)}, S_4^3\}}_{\mathcal{A}_2^*} + \underbrace{\{C_{2(2)}, S_4\}}_{\mathcal{A}_4^*} \tag{22}$$

These cosets are related to the set of assemblies ($\mathcal{A}^*$) in one-to-one fashion so that they correspond to $\mathcal{A}_\alpha^*$ of Fig. 4 when regarded as an ordered set. On the action of $C_{2(3)}$, the cosets are permuted to give $C_{2(3)}I\mathbf{C}_s = C_{2(3)}\mathbf{C}_s (\leftrightarrow \mathcal{A}_3^*)$, $C_{2(3)}C_{2(3)}\mathbf{C}_s = I\mathbf{C}_s (\leftrightarrow \mathcal{A}_1^*)$, $C_{2(3)}C_{2(1)}\mathbf{C}_s = C_{2(2)}\mathbf{C}_s$ $(\leftrightarrow \mathcal{A}_4^*)$, and $C_{2(3)}C_{2(2)}\mathbf{C}_s = C_{2(1)}\mathbf{C}_s (\leftrightarrow \mathcal{A}_2^*)$. The set of these cosets as an ordered set correspond to $\mathcal{A}_\beta^*$ of Fig. 5. Thus, the same permutations as those listed in eqs. 13–20 are obtained by permuting the set of cosets as an ordered set. This is the mathematical way of obtaining CRs. Hence, the permutation representations obtained diagrammatically in the different ways (the present way and the way described in Part 1) can be equalized to CRs.

2.1.3 Assemblies of Other Symmetries

By analogy to the procedure for selecting the orbit of $\mathbf{C}_s$-assemblies described above, respective orbits of assemblies of other symmetries can be constructed, as shown in Table 1. In general, a $\mathbf{G}_j$-assembly represents a $\mathbf{G}_j$-molecule, where $\mathbf{G}_j$ is a subgroup of $\mathbf{G}$. On the action of $\mathbf{G}$, the $\mathbf{G}_j$-assembly is transformed into equivalent $\mathbf{G}_j$-assemblies, which construct an orbit governed by $\mathbf{G}(/\mathbf{G}_j)$.

As an example of chiral subgroups, an orbit of $\mathbf{C}_2'$-assemblies is obtained as follows:

$$\mathcal{B}^* = \{\mathcal{B}_1^*, \mathcal{B}_2^*, \mathcal{B}_3^*, \mathcal{B}_4^*\}. \tag{23}$$

The set $\mathcal{B}^*$ as an ordered set gives a permutation representation, which is equalized to the CR $\mathbf{D}_{2d}(/\mathbf{C}_2')$. The $\mathbf{C}_2'$-assemblies are chiral, while the $\mathbf{C}_s$-assemblies described in the preceding subsection are achiral. Because the symmetries ($\mathbf{C}_2'$ and $\mathbf{C}_s$) appear as the local symmetries in the CRs ($\mathbf{D}_{2d}(/\mathbf{C}_2')$ and $\mathbf{D}_{2d}(/\mathbf{C}_s)$), the sphericities of the orbits governed by the CRs can be understandable as "sphericities in intermolecular stereochemistry (stereoisomerism)", as discussed in the next subsection.

Exercise 2. Apply the procedure exemplified by the orbit of $\mathbf{C}_s$-assemblies (cf. 2.1.2) to the cases listed in Table 1. Compare the results for $\mathcal{A}^*$, $\mathcal{B}^*$, $\mathcal{C}^*$, $\mathcal{D}^*$, $\mathcal{E}^*$, $\mathcal{F}^*$, and $\mathcal{G}^*$ with those for $\mathcal{A}$, $\mathcal{B}$, $\mathcal{C}$, $\mathcal{D}$, $\mathcal{E}$, $\mathcal{F}$, and $\mathcal{G}$ which have been described in Part 1.

---

[9]Strictly speaking, this representation corresponds to left cosets $g^{-1}\mathbf{C}_s$ while eqs. 23–30 of Part 1 corresponds to right cosets $\mathbf{C}_s g$, where g is a representative selected from $\mathbf{D}_{2d}$.

Table 1: Orbits of Assemblies

Symmetry $\mathbf{G}_j$	Orbit governed by the CR $\mathbf{D}_{2d}(/\mathbf{G}_j)$	$\mathbf{G}_j$-Assemblies of Transformulas
$\mathbf{C}_s$	$\mathcal{A}^* = \{\mathcal{A}_1^*, \mathcal{A}_2^*, \mathcal{A}_3^*, \mathcal{A}_4^*\}$	$\mathcal{A}_1^* = \{f_1, f_2\},\ \mathcal{A}_2^* = \{f_7, f_4\},$
		$\mathcal{A}_3^* = \{f_5, f_6\},\ \mathcal{A}_4^* = \{f_3, f_8\}$
$\mathbf{C}_2'$	$\mathcal{B}^* = \{\mathcal{B}_1^*, \mathcal{B}_2^*, \mathcal{B}_3^*, \mathcal{B}_4^*\}$	$\mathcal{B}_1^* = \{f_2, f_7\}\ \mathcal{B}_2^* = \{f_4, f_5\},$
		$\mathcal{B}_3^* = \{f_6, f_3\},\ \mathcal{B}_4^* = \{f_1, f_8\}$
$\mathbf{C}_2$	$\mathcal{C}^* = \{\mathcal{C}_1^*, \mathcal{C}_2^*, \mathcal{C}_3^*, \mathcal{C}_4^*\}$	$\mathcal{C}_1^* = \{f_1, f_5\}\ \mathcal{C}_2^* = \{f_2, f_6\},$
		$\mathcal{C}_3^* = \{f_3, f_7\},\ \mathcal{C}_4^* = \{f_4, f_8\}$
$\mathbf{C}_{2v}$	$\mathcal{D}^* = \{\mathcal{D}_1^*, \mathcal{D}_2^*\}$	$\mathcal{D}_1^* = \{f_1, f_2, f_5, f_6\},\ \mathcal{D}_2^* = \{f_3, f_4, f_7, f_8\}$
$\mathbf{D}_2$	$\mathcal{E}^* = \{\mathcal{E}_1^*, \mathcal{E}_2^*\}$	$\mathcal{E}_1^* = \{f_1, f_4, f_5, f_8\},\ \mathcal{E}_2^* = \{f_2, f_3, f_6, f_7\}$
$\mathbf{S}_4$	$\mathcal{F}^* = \{\mathcal{F}_1^*, \mathcal{F}_2^*\}$	$\mathcal{F}_1^* = \{f_1, f_3, f_5, f_7\},\ \mathcal{F}_2^* = \{f_2, f_4, f_6, f_8\}$
$\mathbf{D}_{2d}$	$\mathcal{G}^* = \{\mathcal{G}_1^*\}$	$\mathcal{G}_1^* = \{f_1, f_2, f_3, f_4, f_5, f_6, f_7, f_8\},$

2.2 Molecules Represented by Assemblies

2.2.1 $\mathbf{C}_1$-Molecules as Special Assemblies

The selection of the $\mathbf{C}_1$-assembly (**1**) is accompanied by the subduction $\mathbf{D}_{2d}(/\mathbf{C}_1) \downarrow \mathbf{C}_1 = 8\mathbf{C}_1(/\mathbf{C}_1)$ with respect to intramolecular stereochemistry described in Part 1. This means that the eight vertices of the $\mathbf{C}_1$-assembly (**1**) are nonequivalent to each other with considering the numbering of the vertices. A $\mathbf{C}_1$-assembly (e.g., **1**) derived from a regular body corresponds to a $\mathbf{C}_1$-molecule. This conclusion can be confirmed by constructing a concrete $\mathbf{C}_1$-molecule, where either one of the vertices is replaced by an object of another kind ($\bullet$), producing **10** as a $\mathbf{C}_1$-molecule.

The resulting $\mathbf{C}_1$-assembly of a transformula, which corresponds to a single $\mathbf{C}_1$-molecule (i.e., **10**), is transformed into the other $\mathbf{C}_1$-assemblies (**11–17**). Because these $\mathbf{C}_1$-assemblies (**11–17**) are equivalent to **10** under the action of $\mathbf{D}_{2d}$, the totally eight $\mathbf{C}_1$-assemblies (**10–17**) construct a $\mathbf{D}_{2d}(/\mathbf{C}_1)$-orbit. The local symmetry $\mathbf{C}_1$ denotes the symmetry of the original transformula (i.e., **10**), which can be regarded as a representative of the $\mathbf{C}_1$-molecule at issue.

2.2.2 $\mathbf{C}_s$-Molecules as Special Assemblies

The $\mathbf{C}_s$-assembly (e.g., $\mathcal{A}_1^* = \{\mathbf{1}, \mathbf{6}\}$ in Fig. 4) corresponds to a $\mathbf{C}_s$-molecule, because it is selected as a fixed object, as represented by a surrounding box.[10] Because the selection of the $\mathbf{C}_s$-assembly is accompanied by the subduction $\mathbf{D}_{2d}(/\mathbf{C}_1) \downarrow \mathbf{C}_s = 4\mathbf{C}_s(/\mathbf{C}_1)$ with respect to intramolecular stereochemistry described in Part 1, the vertices of the regular body are nonequivalent. It follows that two vertices can be selected to be replaced by objects of another kind ($\bullet$), producing a $\mathbf{C}_s$-assembly (e.g., $\mathcal{A}_1^\dagger = \{\mathbf{18}, \mathbf{22}\} = \{f_1^\dagger, f_2^\dagger\}$) shown in Fig. 7. The resulting $\mathbf{C}_s$-assembly $\mathcal{A}_1^\dagger$, which corresponds to a single $\mathbf{C}_s$-molecule (**18** as a representative), is trans-

---

[10]Mathematically speaking, the group $\mathbf{C}_s$ is selected as a stabilizer. The term "fixed" means that the two transformulas surrounded by a box are considered to be identical with each other so as to represent a single molecule.
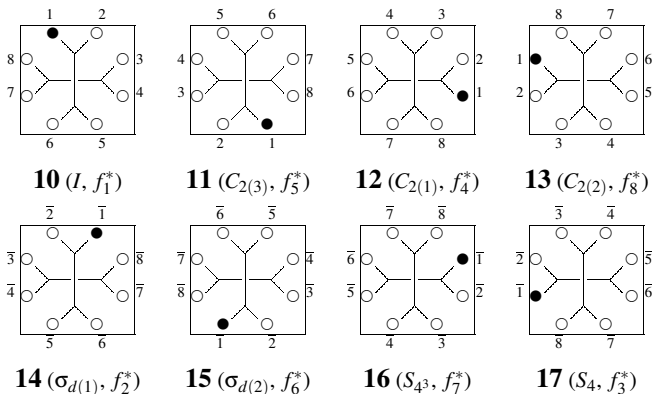
10 (I, f_1^*) **11** $(C_{2(3)}, f_5^*)$ **12** $(C_{2(1)}, f_4^*)$ **13** $(C_{2(2)}, f_8^*)$

14 $(\sigma_{d(1)}, f_2^*)$ **15** $(\sigma_{d(2)}, f_6^*)$ **16** $(S_4{}^3, f_7^*)$ **17** (S_4, f_3^*)

Figure 6: $\mathbf{C}_1$-Molecules corresponding to eight $\mathbf{C}_1$-assemblies (f_1^*–f_8^*), which are equivalent on the action of $\mathbf{D}_{2d}$. Each of the $\mathbf{C}_1$-assemblies consists of one transformula. The alignment shown in this diagram corresponds to an ordered set, $\mathcal{T}_\alpha^* = \{f_1^*, f_5^*, f_4^*, f_8^*, f_2^*, f_6^*, f_7^*, f_3^*\}$, which is an orbit governed by the regular representation $\mathbf{D}_{2d}(/\mathbf{C}_1)$.

formed into the other $\mathbf{C}_s$-assemblies ($\mathcal{A}_3^\dagger = \{\mathbf{19}, \mathbf{23}\} = \{f_5^\dagger, f_6^\dagger\}$, $\mathcal{A}_2^\dagger = \{\mathbf{20}, \mathbf{24}\} = \{f_7^\dagger, f_4^\dagger\}$, and $\mathcal{A}_4^\dagger = \{\mathbf{21}, \mathbf{25}\} = \{f_3^\dagger, f_8^\dagger\}$), as shown in Fig. 7. Because these four $\mathbf{C}_s$-assemblies ($\mathcal{A}_1^\dagger$, $\mathcal{A}_3^\dagger$, $\mathcal{A}_2^\dagger$, and $\mathcal{A}_4^\dagger$) are equivalent to one another under the action of $\mathbf{D}_{2d}$, the four $\mathbf{C}_s$-assemblies construct a $\mathbf{D}_{2d}(/\mathbf{C}_s)$-orbit. The local symmetry $\mathbf{C}_s$ denotes the symmetry of the original transformula (i.e., **18**), which can be regarded as a representative of the $\mathbf{C}_s$-molecule at issue.

2.2.3 Molecules of Other Symmetries as Special Assemblies

The procedure described above for obtaining the CR $\mathbf{D}_{2d}(/\mathbf{C}_s)$ can be extended to a general procedure so that the set of assemblies for representing the CR (Fig. 4, 5, and the other six figures) is replaced by the set of assemblies corresponding to another subgroup. This task is open to the challenge of readers as an exercise:

Exercise 3. Select an assembly of transformulas corresponding to each subgroup $\mathbf{G}_i$ of $\mathbf{D}_{2d}$, where $\mathbf{G}_i = \mathbf{C}_s, \mathbf{C}_2', \mathbf{C}_2, \mathbf{C}_{2v}, \mathbf{D}_2, \mathbf{S}_4$, and $\mathbf{D}_{2d}$. Repeat the procedure described for the CR $\mathbf{D}_{2d}(/\mathbf{C}_s)$ in order to obtain other CRs, i.e., $\mathbf{D}_{2d}(/\mathbf{G}_i)$. Let these orbits (governed by $\mathbf{D}_{2d}(/\mathbf{C}_s)$, $\mathbf{D}_{2d}(/\mathbf{C}_2')$, $\mathbf{D}_{2d}(/\mathbf{C}_2)$, $\mathbf{D}_{2d}(/\mathbf{C}_{2v})$, $\mathbf{D}_{2d}(/\mathbf{D}_2)$, $\mathbf{D}_{2d}(/\mathbf{S}_4)$, and $\mathbf{D}_{2d}(/\mathbf{D}_{2d})$) be represented by the symbols, $\mathcal{A}^\dagger$, $\mathcal{B}^\dagger$, $\mathcal{C}^\dagger$, $\mathcal{D}^\dagger$, $\mathcal{E}^\dagger$, $\mathcal{F}^\dagger$, and $\mathcal{G}^\dagger$. Then compare these orbits with the ones obtained in Exercise 2, i.e., $\mathcal{A}^*$, $\mathcal{B}^*$, $\mathcal{C}^*$, $\mathcal{D}^*$, $\mathcal{E}^*$, $\mathcal{F}^*$, and $\mathcal{G}^*$ (cf. Table 1).

2.2.4 Sphericities in Intermolecular Stereochemistry

The concept of sphericities is also effective to describe intermolecular stereochemistry (stereoisomerism). Because the CR $\mathbf{D}_{2d}(/\mathbf{C}_s)$ is homospheric, the assembles of $\mathcal{A}^* = \{\mathcal{A}_1^*, \mathcal{A}_2^*, \mathcal{A}_3^*, \mathcal{A}_4^*\}$ (Table 1) construct a homospheric orbit. The homospheric orbit $\mathcal{A}^*$ corresponds to the homospheric orbit $\mathcal{A}^\dagger$ (cf. 2.2.2 and Exercise 3) as shown in Fig. 7, so that the orbit represents
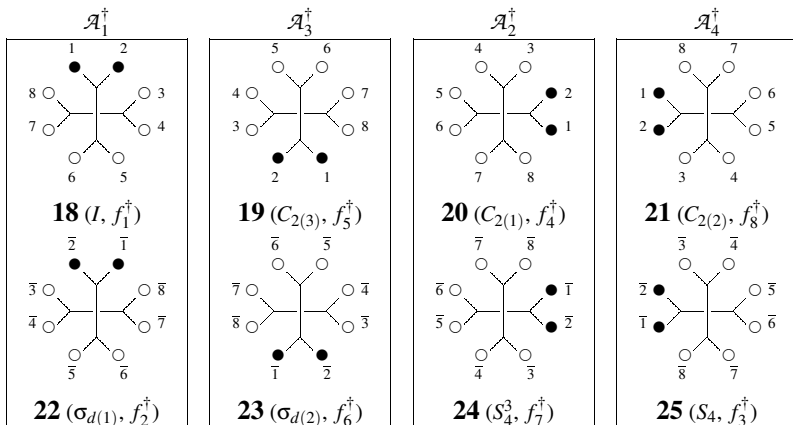
Figure 7: $\mathbf{C}_s$-Molecules corresponding to four $\mathbf{C}_s$-assemblies, i.e., $\mathcal{A}_1^\dagger = \{f_1^\dagger, f_2^\dagger\}$, $\mathcal{A}_2^\dagger = \{f_4^\dagger, f_7^\dagger\}$, $\mathcal{A}_3^\dagger = \{f_5^\dagger, f_6^\dagger\}$, and $\mathcal{A}_4^\dagger = \{f_8^\dagger, f_3^\dagger\}$, which are equivalent on the action of $\mathbf{D}_{2d}$. Each of the $\mathbf{C}_s$-assemblies consists of two transformulas. The alignment shown in this diagram corresponds to an ordered set, $\mathcal{A}_\alpha^\dagger = \{\mathcal{A}_1^\dagger, \mathcal{A}_3^\dagger, \mathcal{A}_2^\dagger, \mathcal{A}_4^\dagger\}$, which is an orbit governed by the CR $\mathbf{D}_{2d}(/\mathbf{C}_s)$.

an achiral $\mathbf{C}_s$-molecule. The same situation is true for the CRs $\mathbf{D}_{2d}(/\mathbf{C}_{2v})$, $\mathbf{D}_{2d}(/\mathbf{S}_4)$, and $\mathbf{D}_{2d}(/\mathbf{D}_{2d})$.

On the other hand, the $\mathbf{C}_2'$-assemblies $\mathcal{B}_1^*$ and $\mathcal{B}_3^*$ selected from $\mathcal{B}^* = \{\mathcal{B}_1^*, \mathcal{B}_2^*, \mathcal{B}_3^*, \mathcal{B}_4^*\}$ are the mirror images of $\mathcal{B}_2^*$ and $\mathcal{B}_4^*$ (Table 1). This corresponds to the fact that the four $\mathbf{C}_2'$-assemblies construct a four-membered $\mathbf{D}_{2d}(/\mathbf{C}_2')$-orbit that is enantiospheric, where the orbit (i.e., $\mathcal{B}^\dagger$ obtained in Exercise 3) represents an enantiomeric pair of chiral $\mathbf{C}_2'$-molecules. The same situation is true for the CRs $\mathbf{D}_{2d}(/\mathbf{C}_2)$ and $\mathbf{D}_{2d}(/\mathbf{D}_2)$.

The hemisphericity appears when a chiral skeleton is taken into consideration. Such a chiral skeleton is accompanied by the chiral skeleton of opposite chirality (i.e., the enantiomeric skeleton). If the enantiomeric skeletons are pairwise considered, they can be discussed in terms of enantiosphericity, even though careful examinations are necessary.

It should be noted that the comparison of the homospheric cases with the enantiospheric cases reveals one of the essential features of Fujita's USCI approach: *A pair of enantiomeric molecules (totally achiral) and an achiral molecule are considered to be in an equal level of consideration. The pair of enantiomeric molecules is characterized by the enantiosphericity in stereoisomerism, while the achiral molecule is characterized by the homosphericity in stereoisomerism.*

2.3 Subductions of Orbits of Assemblies

The concept of *subductions of CRs* works well in discussions on orbits of assemblies. For example, let us consider the subduction of the CR $\mathbf{D}_{2d}(/\mathbf{C}_s) \downarrow \mathbf{C}_s$. This subduction is diagrammatically explained by the selection of two permutations corresponding to $\mathbf{C}_s = \{I, \sigma_{d(1)}\}$ from

the eight permutations of the obit of assemblies $\mathcal{A}^*$ (eq. 11). The selected permutations are shown in Fig. 8, where the top row (containing four assemblies) is the original alignment ($\sim I$) of $\mathcal{A}^*$ and the second row (containing four assemblies) is the alignment after the $\sigma_{d(1)}$ operation.

On the action of the $\sigma_{d(1)}$ operation, the top row of $\mathcal{A}^* = \{\mathcal{A}_1^*, \mathcal{A}_3^*, \mathcal{A}_2^*, \mathcal{A}_4^*\}$ is converted into second row $\mathcal{A}^* = \{\mathcal{A}_1^*, \mathcal{A}_3^*, \mathcal{A}_4^*, \mathcal{A}_2^*\}$. The comparison of the two rows teaches us that $\mathcal{A}_1^*$ (or $\mathcal{A}_3^*$) is fixed on the action of $\mathbf{C}_s$ (i.e., $\mathcal{A}_1^* \to \overline{\mathcal{A}_1^*} \, (= \mathcal{A}_1^*)$ or $\mathcal{A}_3^* \to \overline{\mathcal{A}_3^*} \, (= \mathcal{A}_3^*)$) and that $\mathcal{A}_2^*$ and $\mathcal{A}_4^*$ are exchanged (i.e., $\mathcal{A}_2^* \to \overline{\mathcal{A}_4^*} \, (= \mathcal{A}_4^*)$ and $\mathcal{A}_4^* \to \overline{\mathcal{A}_2^*} \, (= \mathcal{A}_2^*)$). This means that $\mathcal{A}^*$ is divided into two one-membered orbits (i.e., $\{\mathcal{A}_1^*\}$ and $\{\mathcal{A}_3^*\}$) and one two-membered orbit (i.e., $\{\mathcal{A}_2^*, \mathcal{A}_4^*\}$). Because the transformula of the resulting one-membered orbit $\{\mathcal{A}_1^*\}$ (or $\{\mathcal{A}_3^*\}$) is fixed by $\mathbf{C}_s$, it is concluded to be governed by $\mathbf{C}_s(/\mathbf{C}_s)$. Because each transformula of the other two-membered orbit $\{\mathcal{A}_2^*, \mathcal{A}_4^*\}$) is fixed by $\mathbf{C}_1$, it is concluded to be governed by $\mathbf{C}_s(/\mathbf{C}_1)$. Hence, Fig. 8 represents the subduction of the CR $\mathbf{D}_{2d}(/\mathbf{C}_s) \downarrow \mathbf{C}_s = 2\mathbf{C}_s(/\mathbf{C}_s) + \mathbf{C}_s(/\mathbf{C}_1)$. The same result can be obtained by the selection of the permutations shown in eqs. 13 and 17.

Because the $\mathbf{C}_s(/\mathbf{C}_s)$-orbit is a one-membered homospheric orbit and the $\mathbf{C}_s(/\mathbf{C}_1)$-orbit is a two-membered enantiospheric orbit (cf. Table 5 of Part 1), the subduction is characterized by the USCI-CF $a_1^2 c_2$. The corresponding mark is equal to 2 because of the power of the sphericity index a_1.

The subduction procedure is repeated to cover all of the subgroups of $\mathbf{D}_{2d}$, giving the modes of division for the original $\mathbf{D}_{2d}(/\mathbf{C}_s)$-orbit:

Subduction	Result	USCI-CF	USCI	Mark	
$\mathbf{D}_{2d}(/\mathbf{C}_s) \downarrow \mathbf{D}_{2d} = \mathbf{D}_{2d}(/\mathbf{C}_s)$		a_4	s_4	0	(24)
$\mathbf{D}_{2d}(/\mathbf{C}_s) \downarrow \mathbf{D}_2 = \mathbf{D}_2(/\mathbf{C}_1)$		b_4	s_4	0	(25)
$\mathbf{D}_{2d}(/\mathbf{C}_s) \downarrow \mathbf{C}_{2v} = \mathbf{C}_{2v}(/\mathbf{C}_s) + \mathbf{C}_{2v}(/\mathbf{C}_s')$		a_2^2	s_2^2	0	(26)
$\mathbf{D}_{2d}(/\mathbf{C}_s) \downarrow \mathbf{S}_4 = \mathbf{S}_4(/\mathbf{C}_1)$		c_4	s_4	0	(27)
$\mathbf{D}_{2d}(/\mathbf{C}_s) \downarrow \mathbf{C}_s = 2\mathbf{C}_s(/\mathbf{C}_s) + \mathbf{C}_s(/\mathbf{C}_1)$		$a_1^2 c_2$	$s_1^2 s_2$	2	(28)
$\mathbf{D}_{2d}(/\mathbf{C}_s) \downarrow \mathbf{C}_2 = 2\mathbf{C}_2(/\mathbf{C}_1)$		b_2^2	s_2^2	0	(29)
$\mathbf{D}_{2d}(/\mathbf{C}_s) \downarrow \mathbf{C}_2' = 2\mathbf{C}_2'(/\mathbf{C}_1)$		b_2^2	s_2^2	0	(30)
$\mathbf{D}_{2d}(/\mathbf{C}_s) \downarrow \mathbf{C}_1 = 4\mathbf{C}_1(/\mathbf{C}_1)$		b_1^4	s_1^4	4	(31)

The results shown in eqs. 24–31 are equivalent to the ones shown in eqs. 60–67 of Part 1. It should be noted that the $\mathbf{D}_{2d}(/\mathbf{C}_s)$-orbit is characterized by the subductions (eqs. 24–31), by the USCI-CFs ($\{b_1^4, b_2^2, b_2^2, a_1^2 c_2, c_4, a_2^2, b_4, a_4\}$), by the USCIs ($\{s_1^4, s_2^2, s_2^2, s_1^2 s_2, s_4, s_2^2, s_4, s_4\}$), and by the marks ($\{4, 0, 0, 2, 0, 0, 0, 0\}$), where these are aligned in an ascending order of the orders of the subgroups (cf. Tables 8–11 of Part 1).

Exercise 4. Derive eqs. 24–31 diagrammatically by following the procedure given above. Compare the derivation with the one described for obtaining eqs. 60–67 of Part 1.

The above-described procedure can be more clearly demonstrated by considering Fig. 7 for $\mathcal{A}^\dagger$ in place of Fig. 4 for $\mathcal{A}^*$. Among the eight permutation diagrams of the orbit of assemblies $\mathcal{A}^\dagger$, two permutation diagrams corresponding to $\mathbf{C}_s = \{I, \sigma_{d(1)}\}$ are selected, giving Figs. 7 (for I) and 9 (for $\sigma_{d(1)}$), which are gathered to give the counterpart of Fig. 8. By comparing these diagrams, one can find that the $\{\mathcal{A}_1^\dagger\}$ and the $\{\mathcal{A}_3^\dagger\}$ are respectively immobile (fixed or stabilized), while the $\mathcal{A}_2^\dagger$ and the $\mathcal{A}_4^\dagger$ are interchanged into each other. Thus, the symmetry restriction from $\mathbf{D}_{2d}$ to $\mathbf{C}_s$ divides the four-membered orbit ($\mathcal{A}^\dagger$) into two one-membered orbits ($\{\mathcal{A}_1^\dagger\}$ and $\{\mathcal{A}_3^\dagger\}$) and a two-membered orbit($\{\mathcal{A}_2^\dagger, \mathcal{A}_4^\dagger\}$).
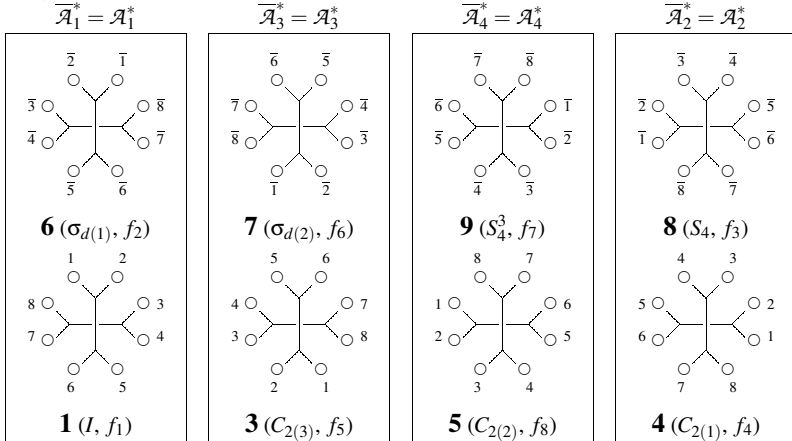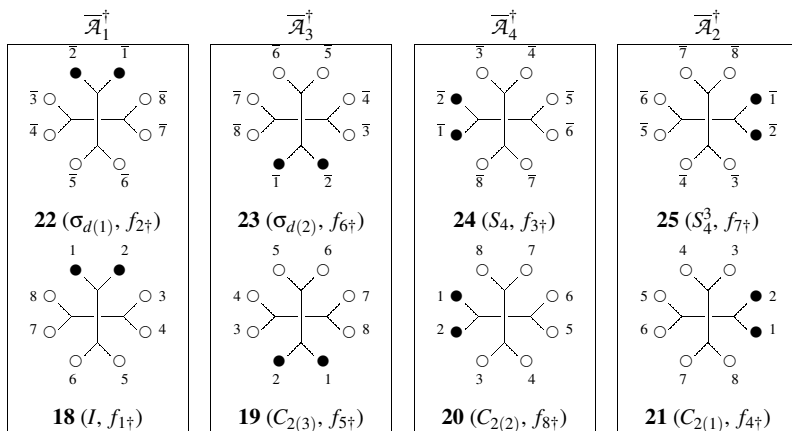
$I \sim$
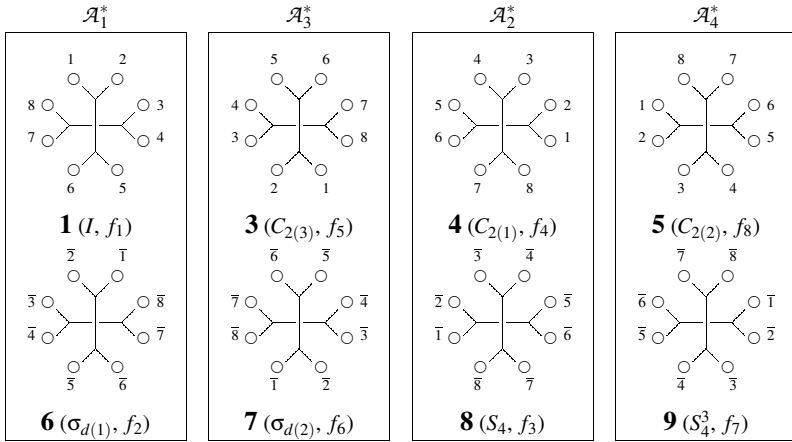
$\sigma_{d(1)} \sim$

Figure 8: Two permutations of the set of assemblies representing the subduction of the CR $\mathbf{D}_{2d}(/\mathbf{C}_s) \downarrow \mathbf{C}_s = 2\mathbf{C}_s(/\mathbf{C}_s) + \mathbf{C}_s(/\mathbf{C}_1)$. The top row of $\mathcal{A}^* = \{\mathcal{A}_1^*, \mathcal{A}_3^*, \mathcal{A}_2^*, \mathcal{A}_4^*\}$ is converted into second row $\mathcal{A}^* = \{\mathcal{A}_1^*, \mathcal{A}_3^*, \mathcal{A}_4^*, \mathcal{A}_2^*\}$, where $\mathcal{A}^*$ is divided into two one-membered orbits (i.e., $\{\mathcal{A}_1^*\}$ and $\{\mathcal{A}_3^*\}$) and one two-membered orbit (i.e., $\{\mathcal{A}_2^*, \mathcal{A}_4^*\}$).

Figure 9: The action of $\sigma_{d(1)}$ on the $\mathbf{C}_s$-molecule (the four $\mathbf{C}_s$-assemblies) listed in Fig. 7. The alignment shown in this diagram corresponds to an ordered set, $\mathcal{A}_\alpha^\dagger = \{\mathcal{A}_1^\dagger, \mathcal{A}_3^\dagger, \mathcal{A}_4^\dagger, \mathcal{A}_2^\dagger\}$.

Because the transformula of the resulting one-membered orbit $\{\mathcal{A}_1^\dagger\}$ (or $\{\mathcal{A}_3^\dagger\}$) is fixed by $\mathbf{C}_s$, it is concluded to be governed by $\mathbf{C}_s(/\mathbf{C}_s)$. Because each transformula of the other two-membered orbit $\{\mathcal{A}_2^\dagger, \mathcal{A}_4^\dagger\}$) is fixed by $\mathbf{C}_1$, it is concluded to be governed by $\mathbf{C}_s(/\mathbf{C}_1)$. This represents the subduction of the CR $\mathbf{D}_{2d}(/\mathbf{C}_s) \downarrow \mathbf{C}_s = 2\mathbf{C}_s(/\mathbf{C}_s) + \mathbf{C}_s(/\mathbf{C}_1)$. Moreover, the corresponding USCI-CF (or USCI) is calculated to be $a_1^2 c_2$ (or $s_1^2 s_2$) and the mark of this restriction is obtained to be equal to 2 (two one-membered orbits). The diagrammatical procedure is repeated to cover all of the symmetry operations of $\mathbf{D}_{2d}$ so that the same subduction table as Table 8 of Part 1, the same USCI-CF table as Table 9 of Part 1, the same USCI table as Table 10 of Part 1, and the same mark table as Table 11 of Part 1 are obtained alternatively.

3 Mandalas as Nested Regular Bodies

The discussions described in Section 2 have essentially followed Chapters 13 and 15 of Fujita's book [10], although a more diagrammatical approach has been adopted by following partly the treatment reported recently [16, 17]. Because the discussions have required eight diagrams of permutations, each of which contains eight transformulas for $\mathbf{D}_{2d}$, a more simplified approach should be developed to take a further discussion. This task can be accomplished by considering nested regular bodies (named *mandalas*), where an assembly of transformulas, which has been defined in Part 1, will be redefined in a more diagrammatical fashion. As a result, the relationship between the intramolecular stereochemistry (Part 1) and the intermolecular stereochemistry (Part 2) can be clearly demonstrated on the basis of the concept of mandalas.

3.1 Intuitive Definition

A *mandala*[11] is defined as a nested regular body in which a transformula derived from a regular body (named a *corona body*) is placed on a vertex of another regular body (named *a base body*), as shown in Fig. 10. The numbering of each vertex and the correspondence to each symmetry operation ($g \in \mathbf{D}_{2d}$) in the corona body are adopted in the same way as Fig. 26 of Part 1, as found in the eight transformulas (corona bodies) of Fig. 10. On the other hand, each vertex of the base body is renumbered in accord with the correspondence to g^{-1}. Thereby, Fig. 2 is converted into a mandala as a nested regular body (Fig. 10). Although the mandala is a hypothetical structure, it diagrammatically integrates the two fields of stereochemistry. Thus, the corona body represents the intramolecular stereochemistry (Part 1), while the base body represents the intermolecular stereochemistry (Part 2).
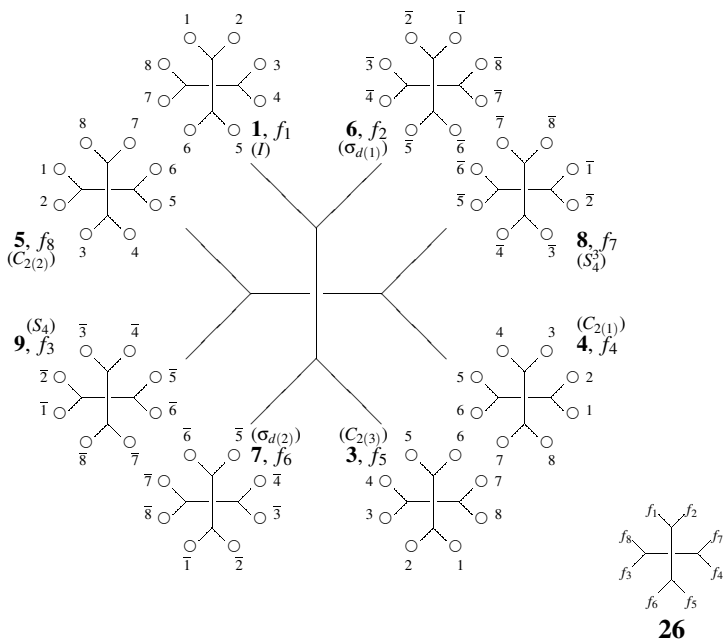

Figure 10: Mandala (a nested regular body) containing eight transformulas (f_1–f_8) at its vertices. The alignment shown in this diagram corresponds to the ordered set shown in Fig. 2, $\mathcal{T}_\alpha = \{f_1, f_5, f_4, f_8, f_2, f_6, f_7, f_3\}$, which is now reordered in a clockwise manner to give $\mathcal{T}'_\alpha = \{f_1, f_2, f_7, f_4, f_5, f_6, f_3, f_8\}$. The full expression of the mandala is simplified into **26**.

The mandala shown in Fig. 10 is simplified by replacing each corona body (transformula) by its symbol (f_1–f_8) so as to give **26** shown in the lower right part of Fig. 10. The action of $C_{2(3)}$

---

[11]The word *mandala* is originally used to denote a circular picture that represents the universe in such eastern religions as Buddhism. The word is here adopted to denote a nested regular body for describing the universe of stereochemistry (the intramolecular and the intermolecular stereochemistry).
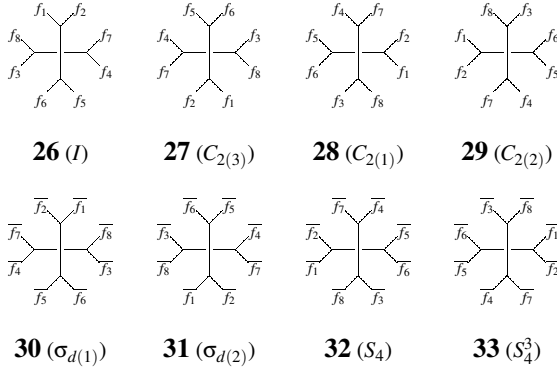
Figure 11: Permutation diagram containing eight mandalas generated by the symmetry operations of $\mathbf{D}_{2d}$. The first mandala (**26**) corresponds to Fig. 2 via Fig. 10. The second one (**27**) corresponds to Fig. 3.

converts **26** (corresponding to Fig. 2 via Fig. 10) into **27**, which is the mandala corresponding to Fig. 3. Thus, all of the symmetry operations of $\mathbf{D}_{2d}$ generate the eight mandalas listed in Fig. 11, which is a permutation diagram of the eight mandalas. Obviously, Fig. 11 represents the same treatment as described in 2.2.1, where the eight sheets (Fig. 2, Fig. 3, and others) used in 2.2.1 are summarized into one sheet (Fig. 11). As a result, the eight mandalas in Fig. 11 correspond to the permutations represented by eqs. 3–10.

Exercise 5. Correlate each mandala of Fig. 11 to each of eqs. 3–10.

3.2 Assemblies in a Mandala

By means of the permutation diagram of mandalas shown in Fig. 11, such assemblies of transformulas as discussed in Subsection 2.1 (Table 1) can be redefined diagrammatically.

3.2.1 Orbits of Assemblies Governed by the CR $\mathbf{D}_{2d}(/\mathbf{C}_s)$

Let us remember the $\mathbf{C}_s$-assemblies shown in Fig. 4. Each assembly contained in the orbit $\mathcal{A}^* = \{\mathcal{A}_1^*, \mathcal{A}_2^*, \mathcal{A}_3^*, \mathcal{A}_4^*\}$ (Fig. 4 and Table 1) is encircled with an oval to generate an assemblage pattern (**34**) shown in Fig. 12. This is depicted as a reference **36** in Fig. 13. Similarly, the $\mathbf{C}_s$-assemblies shown in Fig. 5 generated by the $C_{2(3)}$-operation are diagrammatically represented by **37** in Fig. 13. The above procedure is repeated to cover all of the operations of $\mathbf{D}_{2d}$ so that Fig. 13 is obtained as a permutation diagram for the $\mathbf{C}_s$-assemblies.

The total procedure (Fig. 13) can be diagrammatically considered to be the superposition of the assemblage pattern (**34**) onto the mandalas shown in Fig. 11. Because the orbit $\mathcal{A}^* = \{\mathcal{A}_1^*, \mathcal{A}_2^*, \mathcal{A}_3^*, \mathcal{A}_4^*\}$ in Fig. 13 is the same as the one (eq. 11 and Table 1) described in 2.1.2, the permutation diagram (Fig. 13) generates the same permutations as shown above (eqs. 13–20).

Exercise 6. Correlate each mandala of the permutation diagram (Fig. 13) to each of eqs. 13–20.
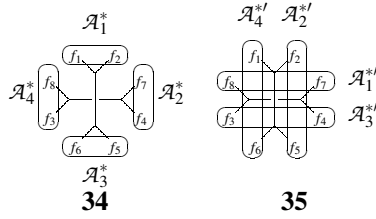
Figure 12: Assemblage patterns to generate orbits of $\mathbf{C}_s$-assemblies in the mandala (**26**). Each assembly encircled by an oval is called a $\mathbf{C}_s$-assembly because it is fixed (stabilized) on the action of $\mathbf{C}_s$ (or its conjugate subgroup $\mathbf{C}_s'$). The resulting set of the four $\mathbf{C}_s$-assemblies is an orbit governed by the CR $\mathbf{D}_{2d}(/\mathbf{C}_s)$.
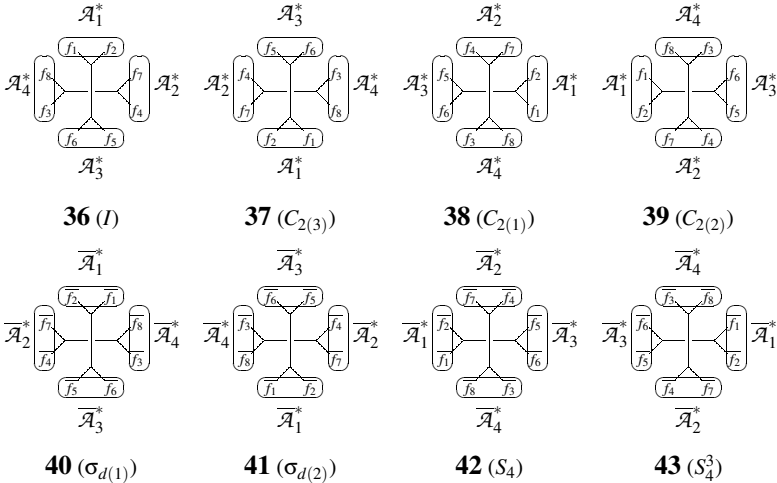

Figure 13: Permutation diagram containing eight mandalas generated by the symmetry operations of $\mathbf{D}_{2d}$. The first mandalas (**26**) corresponds to Fig. 2 via Fig. 10. The second one (**27**) corresponds to Fig. 3. These eight mandalas represent the CR $\mathbf{D}_{2d}(/\mathbf{C}_s)$.

Another assemblage pattern (**35**) shown in Fig. 12 can be selected to construct a permutation diagram, which gives an equivalent CR to the CR $\mathbf{D}_{2d}(/\mathbf{C}_s)$. It should be noted that $\mathbf{C}_s (= \{I, \sigma_{d(1)}\}$ and $\mathbf{C}_s' (= \{I, \sigma_{d(2)}\})$ are conjugate within the group $\mathbf{D}_{2d}$.

Exercise 7. By following the procedure for constructing the permutation diagram (Fig. 13), construct a permutation diagram corresponding to the assemblage pattern (**35**).

3.2.2 Orbits of Assemblies Governed by the CR $\mathbf{D}_{2d}(/\mathbf{C}_2')$

Let us next consider four two-membered sets of transformulas, $\mathcal{B}_1^* = \{f_2, f_7\}$, $\mathcal{B}_2^* = \{f_4, f_5\}$, $\mathcal{B}_3^* = \{f_6, f_3\}$, and $\mathcal{B}_4^* = \{f_1, f_8\}$, which are regarded as assemblies, as shown in **44** of Fig. 14

(cf. Table 1). They are equivalent on the action of operations of $\mathbf{D}_{2d}$ so as to construct an orbit, i.e., $\mathcal{B}^* = \{\mathcal{B}_1^*, \mathcal{B}_2^*, \mathcal{B}_3^*, \mathcal{B}_4^*\}$. Because the assembly $\mathcal{B}_1^*$ is fixed (stabilized) on the action $\mathbf{C}_2'$, the local symmetry of the orbit $\mathcal{B}^*$ is determined to be $\mathbf{C}_2'$. Thereby, the orbit $\mathcal{B}^*$ is concluded to be governed by the CR $\mathbf{D}_{2d}(/\mathbf{C}_2')$. Strictly speaking, the assemblies $\mathcal{B}_1^*$ and $\mathcal{B}_3^*$ are fixed on the action $\mathbf{C}_2' = \{I, C_{2(1)}\}$, while the assemblies $\mathcal{B}_2^*$ and $\mathcal{B}_4^*$ are fixed on the action $\mathbf{C}_2'' = \{I, C_{2(2)}\}$. Because $\mathbf{C}_2'$ and $\mathbf{C}_2''$ are conjugate within $\mathbf{D}_{2d}$, they are regarded as being equivalent in this treatment.
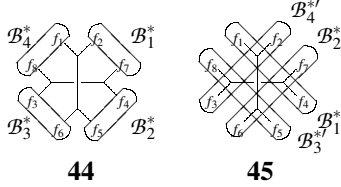

Figure 14: Assemblage patterns to generate orbits of $\mathbf{C}_2'$-assemblies in the mandala Each assembly encircled by an oval is called a $\mathbf{C}_2'$-assembly because it is fixed (stabilized) on the action of $\mathbf{C}_2'$ (or its conjugate subgroup $\mathbf{C}_2''$). The resulting set of the four $\mathbf{C}_2'$-assemblies is an orbit governed by the CR $\mathbf{D}_{2d}(/\mathbf{C}_2')$.

The action of each operation of $\mathbf{D}_{2d}$ causes a permutation of the four assemblies of $\mathcal{B}^*$ (**44**). The result can be summarized to give such a permutation diagram as shown in Fig. 15. The total procedure (Fig. 15) can be diagrammatically considered to be the superposition of the assemblage pattern (**44**) onto the mandalas shown in Fig. 13. Because the orbit $\mathcal{B}^* = \{\mathcal{B}_1^*, \mathcal{B}_2^*, \mathcal{B}_3^*, \mathcal{A}_4^*\}$ in Fig. 15 is the same as the one (Table 1) described in 2.1.2, the permutation diagram (Fig. 15) generates the same permutations, as shown below (eqs. 32–39).

$$I \sim \begin{pmatrix} \mathcal{B}_1^* & \mathcal{B}_2^* & \mathcal{B}_3^* & \mathcal{B}_4^* \\ \mathcal{B}_1^* & \mathcal{B}_2^* & \mathcal{B}_3^* & \mathcal{B}_4^* \end{pmatrix} \sim (1)(2)(3)(4) \tag{32}$$

$$C_{2(3)} \sim \begin{pmatrix} \mathcal{B}_1^* & \mathcal{B}_2^* & \mathcal{B}_3^* & \mathcal{B}_4^* \\ \mathcal{B}_3^* & \mathcal{B}_4^* & \mathcal{B}_1^* & \mathcal{B}_2^* \end{pmatrix} \sim (1\,3)(2\,4) \tag{33}$$

$$C_{2(1)} \sim \begin{pmatrix} \mathcal{B}_1^* & \mathcal{B}_2^* & \mathcal{B}_3^* & \mathcal{B}_4^* \\ \mathcal{B}_1^* & \mathcal{B}_4^* & \mathcal{B}_3^* & \mathcal{B}_2^* \end{pmatrix} \sim (1)(2\,4)(3) \tag{34}$$

$$C_{2(2)} \sim \begin{pmatrix} \mathcal{B}_1^* & \mathcal{B}_2^* & \mathcal{B}_3^* & \mathcal{B}_4^* \\ \mathcal{B}_3^* & \mathcal{B}_2^* & \mathcal{B}_1^* & \mathcal{B}_4^* \end{pmatrix} \sim (1\,3)(2)(4) \tag{35}$$

$$\sigma_{d(1)} \sim \begin{pmatrix} \mathcal{B}_1^* & \mathcal{B}_2^* & \mathcal{B}_3^* & \mathcal{B}_4^* \\ \overline{\mathcal{B}_4^*} & \overline{\mathcal{B}_3^*} & \overline{\mathcal{B}_1^*} & \overline{\mathcal{B}_1^*} \end{pmatrix} \sim \overline{(1\,4)(2\,3)} \tag{36}$$

$$\sigma_{d(2)} \sim \begin{pmatrix} \mathcal{B}_1^* & \mathcal{B}_2^* & \mathcal{B}_3^* & \mathcal{B}_4^* \\ \overline{\mathcal{B}_2^*} & \overline{\mathcal{B}_1^*} & \overline{\mathcal{B}_4^*} & \overline{\mathcal{B}_3^*} \end{pmatrix} \sim \overline{(1\,2)(3\,4)} \tag{37}$$

$$S_4 \sim \begin{pmatrix} \mathcal{B}_1^* & \mathcal{B}_2^* & \mathcal{B}_3^* & \mathcal{B}_4^* \\ \overline{\mathcal{B}_2^*} & \overline{\mathcal{B}_3^*} & \overline{\mathcal{B}_4^*} & \overline{\mathcal{B}_1^*} \end{pmatrix} \sim \overline{(1\,2\,3\,4)} \tag{38}$$

$$S_4^3 \sim \begin{pmatrix} \mathcal{B}_1^* & \mathcal{B}_2^* & \mathcal{B}_3^* & \mathcal{B}_4^* \\ \overline{\mathcal{B}_4^*} & \overline{\mathcal{B}_1^*} & \overline{\mathcal{B}_2^*} & \overline{\mathcal{B}_3^*} \end{pmatrix} \sim \overline{(1\,4\,3\,2)}. \tag{39}$$

46 (I)   **47** ($C_{2(3)}$)   **48** ($C_{2(1)}$)   **49** ($C_{2(2)}$)

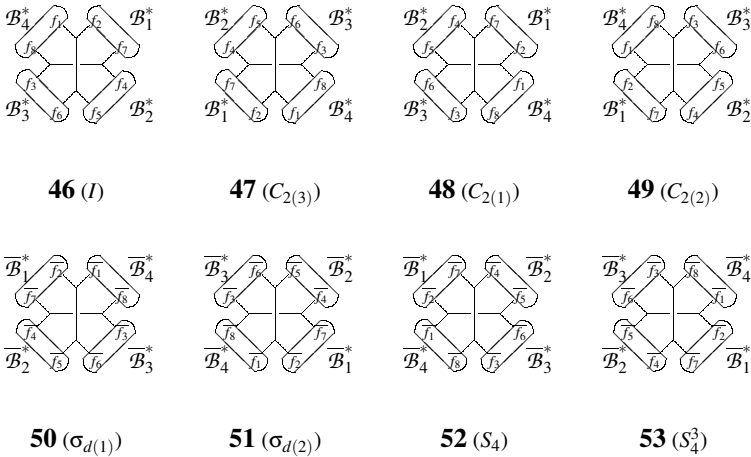**50** ($\sigma_{d(1)}$)   **51** ($\sigma_{d(2)}$)   **52** (S_4)   **53** (S_4^3)

Figure 15: Permutation diagram containing eight mandalas generated by the symmetry operations of $\mathbf{D}_{2d}$. These eight mandalas represent the CR $\mathbf{D}_{2d}(/\mathbf{C}_2')$.

The set of the permutations (eqs. 32—39) is a concrete form of the CR $\mathbf{D}_{2d}(/\mathbf{C}_2')$, which is equivalent to the corresponding CR which has been algebraically obtained by using a coset decomposition of $\mathbf{D}_{2d}$ by $\mathbf{C}_2'$, as discussed generally in Chapter 7 of Fujita's book [10]. Moreover, they are equivalent to the corresponding CR (eqs. 31–38) described in Part 1. Because $\mathbf{D}_{2d}$ is achiral and $\mathbf{C}_2'$ is chiral, a $\mathbf{D}_{2d}(/\mathbf{C}_2')$-orbit is enantiospheric. This CR corresponds to a sphericity index c_4 because of $|\mathbf{D}_{2d}|/|\mathbf{C}_2'| = 8/2 = 4$.

The right assemblage pattern (**45**) of Fig. 14 shows another orbit of assemblies governed by the CR $\mathbf{D}_{2d}(/\mathbf{C}_2')$, i.e., $\mathcal{B}^{*\prime} = \{\mathcal{B}_1^{*\prime}, \mathcal{B}_2^{*\prime}, \mathcal{B}_3^{*\prime}, \mathcal{B}_4^{*\prime}\}$, where we place $\mathcal{B}_1^{*\prime} = \{1, 4\}$, and $\mathcal{B}_2^{*\prime} = \{7, 6\}$, $\mathcal{B}_3^{*\prime} = \{5, 8\}$. $\mathcal{B}_4^{*\prime} = \{2, 3\}$. The assemblies $\mathcal{B}_1^{*\prime}$ and $\mathcal{B}_3^{*\prime}$ are fixed on the action of $\mathbf{C}_2'$, while the assemblies $\mathcal{B}_2^{*\prime}$ and $\mathcal{B}_4^{*\prime}$ are fixed on the action of $\mathbf{C}_2''$, where $\mathbf{C}_2'$ and $\mathbf{C}_2''$ are conjugate within $\mathbf{D}_{2d}$.

Exercise 8. Construct a permutation diagram for the orbit $\mathcal{B}^{*\prime}$ by using the assemblage pattern **45** (Fig. 14). Then, show permutations corresponding to the orbit $\mathcal{B}^{*\prime}$. Compare these permutations with eqs. 32–39.

3.2.3   Orbits of Assemblies Governed by the CR $\mathbf{D}_{2d}(/\mathbf{C}_2)$

The four assemblies of transformulas in **54** of Fig. 16, i.e., $\mathcal{C}_1^* = \{f_1, f_5\}$, $\mathcal{C}_2^* = \{f_2, f_6\}$, $\mathcal{C}_3^* = \{f_3, f_7\}$, and $\mathcal{C}_4^* = \{f_4, f_8\}$, are equivalent on the action of operations of $\mathbf{D}_{2d}$ so that they construct an orbit, i.e., $\mathcal{C}^* = \{\mathcal{C}_1^*, \mathcal{C}_2^*, \mathcal{C}_3^*, \mathcal{C}_4^*\}$. Because the assembly $\mathcal{C}_1^*$ is fixed (stabilized) on the action $\mathbf{C}_2$, the local symmetry of the orbit $\mathcal{C}$ is determined to be $\mathbf{C}_2$. Thereby, the orbit $\mathcal{C}^*$ is concluded to be governed by the CR $\mathbf{D}_{2d}(/\mathbf{C}_2)$.

The action of each operation of $\mathbf{D}_{2d}$ causes a permutation of the four assemblies of $\mathcal{C}$ (**54**) so that the result is represented as such a permutation diagram as shown in Fig. 17. The total
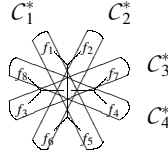
54

Figure 16: Assemblage pattern to generate an orbit of $\mathbf{C}_2$-assemblies in the mandala. Each assembly encircled by an oval is called a $\mathbf{C}_2$-assembly because it is fixed (stabilized) on the action of $\mathbf{C}_2$. The resulting set of the four $\mathbf{C}_2$-assemblies is an orbit governed by the CR $\mathbf{D}_{2d}(/\mathbf{C}_2)$.
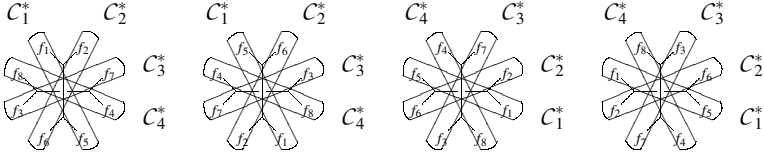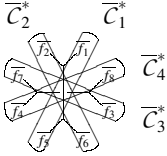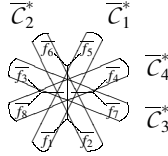

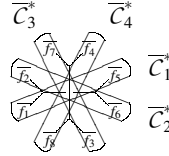**55** (I) **56** ($C_{2(3)}$) **57** ($C_{2(1)}$) **58** ($C_{2(2)}$)
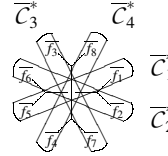

59 ($\sigma_{d(1)}$) **60** ($\sigma_{d(2)}$) **61** (S_4) **62** (S_4^3)

Figure 17: Permutation diagram containing eight mandalas generated by the symmetry operations of $\mathbf{D}_{2d}$. These eight mandalas represent the CR $\mathbf{D}_{2d}(/\mathbf{C}_2)$.

procedure (Fig. 17) can be diagrammatically considered to be the superposition of the assemblage pattern (**54**) onto the mandalas shown in Fig. 13. The orbit $\mathcal{C}^* = \{C_1^*, C_2^*, C_3^*, C_4^*\}$ in Fig. 17 is the same as the one (Table 1) described in 2.1.2.

The permutation diagram (Fig. 17) gives the following permutations (as products of cycles) for the respective operations:

$$I, C_{2(3)} \sim \begin{pmatrix} C_1^* & C_2^* & C_3^* & C_4^* \\ C_1^* & C_2^* & C_3^* & C_4^* \end{pmatrix} \sim (1)(2)(3)(4) \tag{40}$$

$$C_{2(1)}, C_{2(2)} \sim \begin{pmatrix} C_1^* & C_2^* & C_3^* & C_4^* \\ C_4^* & C_3^* & C_2^* & C_1^* \end{pmatrix} \sim (1\ 4)(2\ 3) \tag{41}$$

$$\sigma_{d(1)}, \sigma_{d(2)} \sim \begin{pmatrix} C_1^* & C_2^* & C_3^* & C_4^* \\ \overline{C}_2 & \overline{C}_1 & \overline{C}_4 & \overline{C}_3 \end{pmatrix} = \overline{(1\ 2)(3\ 4)} \tag{42}$$

$$S_4, S_4^3 \sim \begin{pmatrix} C_1^* & C_2^* & C_3^* & C_4^* \\ C_3 & C_4 & C_1 & C_2 \end{pmatrix} \sim \overline{(1\ 3)(2\ 4)} \tag{43}$$

The set of the permutations (eqs. 40—43) is a concrete form of the CR $\mathbf{D}_{2d}(/\mathbf{C}_2)$, which is equivalent to the corresponding CR which has been algebraically obtained by using a coset decomposition of $\mathbf{D}_{2d}$ by $\mathbf{C}_2$, as discussed generally in Chapter 7 of Fujita's book [10]. Moreover, they are equivalent to the corresponding CR (eqs. 39–42) described in Part 1. Because $\mathbf{D}_{2d}$ is achiral and $\mathbf{C}_2$ is chiral, a $\mathbf{D}_{2d}(/\mathbf{C}_2)$-orbit is enantiospheric. This CR corresponds to a sphericity index c_4 because of $|\mathbf{D}_{2d}|/|\mathbf{C}_2| = 8/2 = 4$.

3.2.4 Orbits of Assemblies Governed by the CR $\mathbf{D}_{2d}(/\mathbf{C}_{2v})$

The two four-membered sets of assemblies in **63** of Fig. 18, i.e., $\mathcal{D}_1^* = \{f_1, f_2, f_5, f_6\}$ and $\mathcal{D}_2^* = \{f_3, f_4, f_7, f_8\}$, are equivalent on the action of operations of $\mathbf{D}_{2d}$ so that they construct an orbit, i.e., $\mathcal{D}^* = \{\mathcal{D}_1^*, \mathcal{D}_2^*\}$. Because the assembly $\mathcal{D}_1^*$ is fixed (stabilized) on the action $\mathbf{C}_{2v}$, the local symmetry of the orbit $\mathcal{D}^*$ is determined to be $\mathbf{C}_{2v}$. Thereby, the orbit $\mathcal{D}^*$ is concluded to be governed by the CR $\mathbf{D}_{2d}(/\mathbf{C}_{2v})$.
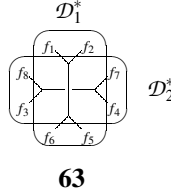

63

Figure 18: Assemblage pattern to generate an orbit of $\mathbf{C}_{2v}$-assemblies in the regular body for illustrating the CR $\mathbf{D}_{2d}(/\mathbf{C}_{2v})$.

The action of each operation of $\mathbf{D}_{2d}$ causes a permutation of the two assemblies of $\mathcal{D}^*$ (**63**). Hence, the total results are represented as such a permutation diagram as shown in Fig. 19. The total procedure (Fig. 19) can be diagrammatically considered to be the superposition of the assemblage pattern (**63**) onto the mandalas shown in Fig. 13. The orbit $\mathcal{D}^* = \{\mathcal{D}_1^*, \mathcal{D}_2^*\}$ in Fig. 19 is the same as the one (Table 1) described in 2.1.2.

By means of the permutation diagram shown in Fig. 19, we can obtain the following permutations (as products of cycles) for the respective operations:

$$I, C_{2(3)} \sim \begin{pmatrix} \mathcal{D}_1^* & \mathcal{D}_2^* \\ \mathcal{D}_1^* & \mathcal{D}_2^* \end{pmatrix} \sim (1)(2) \tag{44}$$

$$C_{2(1)}, C_{2(2)} \sim \begin{pmatrix} \mathcal{D}_1^* & \mathcal{D}_2^* \\ \mathcal{D}_2^* & \mathcal{D}_1^* \end{pmatrix} \sim (1\ 2) \tag{45}$$

$$\sigma_{d(1)}, \sigma_{d(2)} \sim \begin{pmatrix} \mathcal{D}_1^* & \mathcal{D}_2^* \\ \mathcal{D}_1^* & \mathcal{D}_2^* \end{pmatrix} \sim \overline{(1)(2)} \tag{46}$$

$$S_4, S_4^3 \sim \begin{pmatrix} \mathcal{D}_1^* & \mathcal{D}_2^* \\ \mathcal{D}_2^* & \mathcal{D}_1^* \end{pmatrix} \sim \overline{(1\ 2)} \tag{47}$$

The set of the permutations (eqs. 44—47) is a concrete form of the CR $\mathbf{D}_{2d}(/\mathbf{C}_{2v})$, which is equivalent to the corresponding CR which has been algebraically obtained by using a coset decomposition of $\mathbf{D}_{2d}$ by $\mathbf{C}_{2v}$, as discussed generally in Chapter 7 of Fujita's book [10]. Moreover,

64 (I)   **65** ($C_{2(3)}$)   **66** ($C_{2(1)}$)   **67** ($C_{2(2)}$)

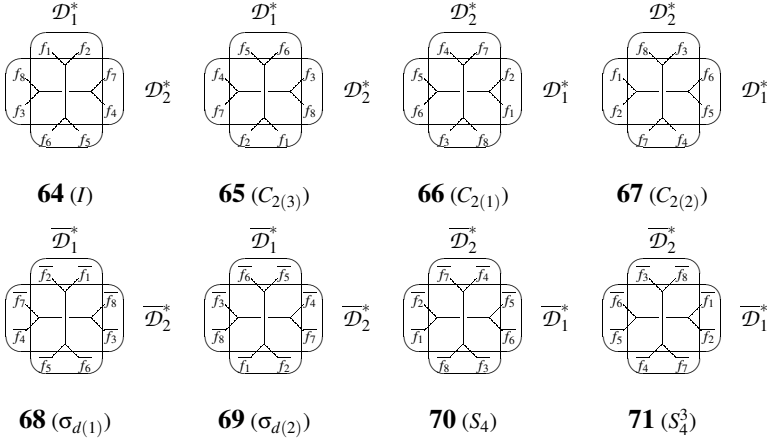**68** ($\sigma_{d(1)}$)   **69** ($\sigma_{d(2)}$)   **70** (S_4)   **71** (S_4^3)

Figure 19: Permutation diagram containing eight mandalas generated by the symmetry operations of $\mathbf{D}_{2d}$. These eight mandalas represent the CR $\mathbf{D}_{2d}(/\mathbf{C}_{2v})$.

they are equivalent to the corresponding CR (eqs. 43–46) described in Part 1. Because both $\mathbf{D}_{2d}$ and $\mathbf{C}_{2v}$ is achiral, a $\mathbf{D}_{2d}(/\mathbf{C}_{2v})$-orbit is homospheric. This CR corresponds to a sphericity index a_2 because of $|\mathbf{D}_{2d}|/|\mathbf{C}_{2v}| = 8/4 = 2$.

3.2.5   Orbits of Assemblies Governed by the Other CRs

The other CRs corresponding to the remaining orbits of assemblies (Table 1) can be obtained similarly. Their derivation is open to the challenge of readers as follows:

Exercise 9. Show an assemblage pattern for $\mathbf{D}_2$-assemblies. Construct the corresponding permutation diagram. Show the concrete forms of the permutations contained in the CR $\mathbf{D}_{2d}(/\mathbf{D}_2)$ (cf. Table 1). Compare them with eqs. 47 and 48 of Part 1.

Exercise 10. Show an assemblage pattern for $\mathbf{S}_4$-assemblies. Construct the corresponding permutation diagram. Show the concrete forms of the permutations contained in the CR $\mathbf{D}_{2d}(/\mathbf{S}_4)$ (cf. Table 1). Compare them with eqs. 49–52 of Part 1.

Exercise 11. Show an assemblage pattern for a $\mathbf{D}_{2d}$-assembly (a trivial case). Construct the corresponding permutation diagram. Show the concrete forms of the permutations contained in the CR $\mathbf{D}_{2d}(/\mathbf{D}_{2d})$ (cf. Table 1). Compare them with eqs. 53 and 54 of Part 1.

3.3   Subductions by Using Mandalas

3.3.1   Subductions of an Orbit of Assemblies in a Mandala

The subductions of orbits of assemblies have been discussed in Subsection 2.3. They can be restated by using mandalas. For example, the subduction $\mathbf{D}_{2d}(/\mathbf{C}_s) \downarrow \mathbf{C}_s$ corresponds to the selection of two mandalas (**36** and **40** in accord with $\mathbf{C}_s = \{I, \sigma_{d(1)}\}$) from the permutation

diagram of mandalas (Fig. 13), which gives Fig. 20. It should be noted that Fig. 20 (**36** for *I* and **40** for $\sigma_{d(1)}$) represents the same selection as depicted in Fig. 8 (the top row for *I* and the second row for $\sigma_{d(1)}$). Obviously, the same results as shown in eq. 28 are obtained from the data of Fig. 20. In accord with the occurrence of two one-membered orbits ($\{\mathcal{A}_1^*\}$ and $\{\mathcal{A}_3^*\}$) and one two-membered orbit ($\{\mathcal{A}_2^*, \mathcal{A}_4^*\}$), we obtain the subduction $\mathbf{D}_{2d}(/\mathbf{C}_s) \downarrow \mathbf{C}_s = 2\mathbf{C}_s(/\mathbf{C}_s) + \mathbf{C}_s(/\mathbf{C}_1)$, the USCI-CF $a_1^2 c_2$, the USCI $s_1^2 s_2$, and the mark 2.
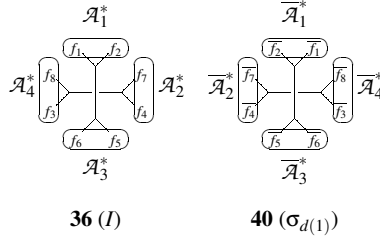

36 (*I*)   **40** ($\sigma_{d(1)}$)

Figure 20: Subduction of a $\mathbf{D}_{2d}(/\mathbf{C}_s)$-orbit into $\mathbf{C}_s$, where **36** and **40** are selected from the permutation diagram of mandalas (Fig. 13).

From the permutation diagram of mandalas (Fig. 13), the mandalas corresponding to a subgroup **H** of $\mathbf{D}_{2d}$ are selected so as to represent the subduction $\mathbf{D}_{2d}(/\mathbf{C}_s) \downarrow \mathbf{H}$ diagrammatically. Because these processes are essentially the same as described in Subsection 2.3, the same results as shown in eqs. 24–31 are obtained. This means that the $\mathbf{D}_{2d}(/\mathbf{C}_s)$-orbit is characterized by the subductions (eqs. 24–31), by the USCI-CFs ($\{b_1^4, b_2^2, b_2^2, a_1^2 c_2, c_4, a_2^2, b_4, a_4\}$), by the USCIs ($\{s_1^4, s_2^2, s_2^2, s_1^2 s_2, s_4, s_2^2, s_4, s_4\}$), and by the marks ($\{4,0,0,2,0,0,0,0\}$). These data are equal to the $\mathbf{D}_{2d}(/\mathbf{C}_s)$-row of the respective tables reported in Part 1 (Tables 8–11).

3.3.2 Tables of Fujita's USCI approach

By following the procedure described above, tables for Fujita's USCI approach (i.e., subduction tables, USCI-CF tables, USCI tables, and mark tables [10]) can be obtained by starting from a permutation diagram of mandalas (e.g., Fig. 13 for $\mathbf{D}_{2d}(/\mathbf{C}_s)$). Thereby, the same tables as Tables 8–11 of Part 1 can be obtained in an alternative way. The task of obtaining them is left to readers as the following exercises:

Exercise 12. By using the permutation diagram for $\mathbf{D}_{2d}(/\mathbf{C}_2')$ (Fig. 15), derive the subduction $\mathbf{D}_{2d}(/\mathbf{C}_2') \downarrow \mathbf{H}$, where **H** runs to cover all the subgroups of $\mathbf{D}_{2d}$.

Exercise 13. By using the permutation diagram for $\mathbf{D}_{2d}(/\mathbf{C}_2)$ (Fig. 17), derive the subduction $\mathbf{D}_{2d}(/\mathbf{C}_2) \downarrow \mathbf{H}$, where **H** runs to cover all the subgroups of $\mathbf{D}_{2d}$.

Exercise 14. By using the permutation diagram for $\mathbf{D}_{2d}(/\mathbf{C}_{2v})$ (Fig. 19), derive the subduction $\mathbf{D}_{2d}(/\mathbf{C}_{2v}) \downarrow \mathbf{H}$, where **H** runs to cover all the subgroups of $\mathbf{D}_{2d}$.

Exercise 15. Construct the subduction table, the USCI-CF table, the USCI table, and the mark table for $\mathbf{D}_{2d}$.

4 Intermolecular and Intramolecular Stereochemistry

4.1 Common Theoretical Framework

Part 1 shows that an orbit of segments in a regular body of **G**-symmetry corresponds to an orbit of (pro)ligands (or atoms) through a CR **G(/H)**, where each (pro)ligand (or atom) belongs to **H**-symmetry from the intramolecular view of stereochemistry. On the other hand, Part 2 (the present paper) shows that an orbit of assemblies in a mandala (a nested regular body) of **G**-symmetry corresponds to an orbit of molecules[12] through a CR **G(/H)**, where each molecule belongs to **H**-symmetry from the intermolecular view of stereochemistry (stereoisomerism). In other words, the CR **G(/H)** as a common theoretical framework governs both the intramolecular stereochemistry and the intermolecular stereochemistry. This feature is depicted in Fig. 21 with respect to $\mathbf{D}_{2d}$ as the first example of showing the common theoretical framework.

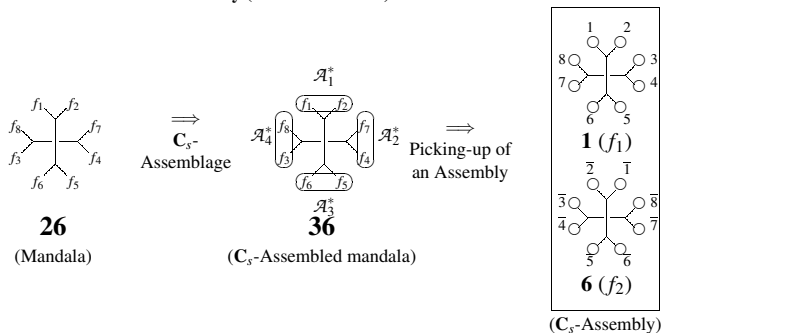As found in Fig. 21, a stepwise procedure for generating a molecule of a given symmetry can be shown as follows:

1. Select a mandala (e.g., **26** or equivalently Fig. 10). The mandala is accompanied with the corresponding permutation diagram (Fig. 11).

2. Select assemblies of a given subsymmetry ($\mathbf{C}_s$) by using an assemblage pattern (**34**), which gives an assembled mandala (**36**). The assembled mandala is accompanied with corresponding permutation diagram (Fig. 13), which shows the CR $\mathbf{D}_{2d}(/\mathbf{C}_s)$.

3. Select an assembly (**1/6**). Because the assembly belong to $\mathbf{C}_s$, the vertices are divided into four orbits: $\{1,2\}$, $\{3,8\}$, $\{4,7\}$, and $\{5,6\}$.

4. According to the division, place (pro)ligands or atoms (○ or ●) on the vertices of the assembly. Thereby, the assembly (**1/6**) corresponds to every molecules (**18**, **72–76**).

5. The vertices of each of the molecules (**18**, **72**, …, or **76**) can be further segmented to give a segmented $\mathbf{C}_s$-molecule (**77**, …, or **82**).

6. Replace each segment in the segmented $\mathbf{C}_s$-molecule (**77**, …, or **82**) by (pro)ligands (or atoms). Thereby, the corresponding $\mathbf{C}_s$-molecule (**83**, …, or **88**) is generated on the basis of an allene skeleton.

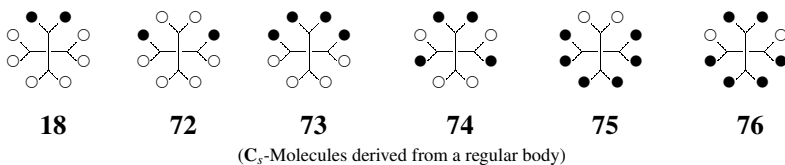By the inspection of Fig. 21, one can find the following remarkable results:

1. The $\mathbf{C}_s$-assembly $\mathcal{A}_1^*$ (= $\{f_1, f_2\}$, i.e., **1/6**) and equivalent assemblies (under $\mathbf{D}_{2d}$) construct a four-membered orbit ($\mathbf{A}^* = \{\mathcal{A}_1^*, \mathcal{A}_2^*, \mathcal{A}_3^*, \mathcal{A}_4^*\}$) governed by $\mathbf{D}_{2d}(/\mathbf{C}_s)$. Each one of the molecules (**18**, **72–76**) exhibits the symmetrically same behavior as $\mathcal{A}_1^*$. For example, the molecule **18** and equivalent molecules (under $\mathbf{D}_{2d}$) construct a four-membered orbit governed by $\mathbf{D}_{2d}(/\mathbf{C}_s)$.

2. Moreover, each one of the segmented $\mathbf{C}_s$-molecules (**77–82**) exhibits the symmetrically same behavior as $\mathcal{A}_1^*$. For example, the segmented molecule **77** and equivalent molecules (under $\mathbf{D}_{2d}$) construct a four-membered orbit governed by $\mathbf{D}_{2d}(/\mathbf{C}_s)$.

---

[12]Strictly speaking, an **H**-assembly of transformulas in a mandala corresponds to a **H**-molecule. Such assemblies as being equivalent to the **H**-assembly under **G**-symmetry constructs an orbit of the **H**-assemblies, which is governed by the **G(/H)**. Hence, **H**-molecules equivalent to the **H**-molecule under **G**-symmetry construct an orbit of the **H**-molecules, which is governed by the **G(/H)**.
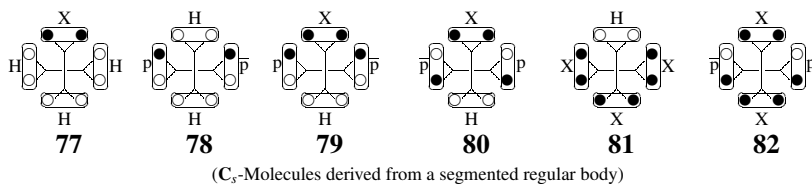
Intermolecular Stereochemistry (Stereoisomerism)

26
(Mandala)

$\mathbf{C}_s$-
Assemblage $\Longrightarrow$

36
($\mathbf{C}_s$-Assembled mandala)

Picking-up of
an Assembly $\Longrightarrow$

1 (f_1)

6 (f_2)

($\mathbf{C}_s$-Assembly)

Assembly into a Molecule $\Downarrow$

18   **72**   **73**   **74**   **75**   **76**

($\mathbf{C}_s$-Molecules derived from a regular body)

Intramolecular Stereochemistry

$\Downarrow$ $\mathbf{C}_s$-Segmentation

77   **78**   **79**   **80**   **81**   **82**

($\mathbf{C}_s$-Molecules derived from a segmented regular body)

$\Downarrow$ Segments into (Pro)lignds (or Atoms)

83   **84**   **85**   **86**   **87**   **88**

($\mathbf{C}_s$-Molecules derived from an allene skeleton)
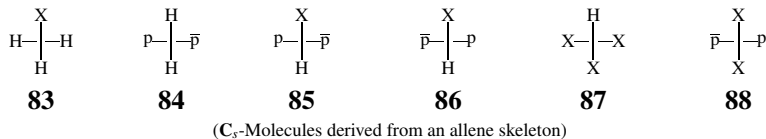
Figure 21: Mandala for $\mathbf{D}_{2d}$, an assembled mandala with a $\mathbf{D}_{2d}(/\mathbf{C}_s)$-orbit of $\mathbf{C}_s$-assemblies, a $\mathbf{C}_s$-assembly selected, $\mathbf{C}_s$-molecules derived from a regular body, $\mathbf{C}_s$-molecules derived from a segmented regular body and $\mathbf{C}_s$-molecules derived from an allene skeleton.

3. Further, each one of the $\mathbf{C}_s$-molecules (**83–88**) exhibits the symmetrically same behavior as $\mathcal{A}_1^*$. For example, the molecule **83** and equivalent molecules (under $\mathbf{D}_{2d}$) construct a four-membered orbit governed by $\mathbf{D}_{2d}(/\mathbf{C}_s)$.

As the second example of showing the common theoretical framework, Fig. 22 shows the participation of a $\mathbf{D}_{2d}(/\mathbf{C}_2')$-orbit in the intermolecular stereochemistry (an orbit of $\mathbf{C}_2'$-assemblies) and that of a $\mathbf{D}_{2d}(/\mathbf{C}_s)$-orbit in the intramolecular stereochemistry (an orbit of $\mathbf{C}_s$-segments)

The stepwise procedure for generating a molecule of a given symmetry (see above) can be also applied to Fig. 22, where the same mandala (e.g., **26** or equivalently Fig. 10) is selected to give the corresponding permutation diagram (Fig. 11). Then, the selection of assemblies of a given subsymmetry ($\mathbf{C}_2'$) by using an assemblage pattern (**45**) gives an assembled mandala, where **45**, though the same expression is used, is now regarded as a reference assembled mandala. The assembled mandala (**45**) is accompanied with corresponding permutation diagram (cf. Fig. 15), which shows the equivalence of the four assemblies ($\mathcal{B}_1^{*\prime}$, $\mathcal{B}_2^{*\prime}$, $\mathcal{B}_3^{*\prime}$, $\mathcal{B}_4^{*\prime}$). This means that the assemblies in the assembled mandala (**45**) construct an orbit represented by $\mathcal{B}^{*\prime} = \{\mathcal{B}_1^{*\prime}, \mathcal{B}_2^{*\prime}, \mathcal{B}_3^{*\prime}, \mathcal{B}_4^{*\prime}\}$. Because the local symmetry of the assembly ($\mathcal{B}_1^{*\prime}$) is $\mathbf{C}_2'$, the orbit ($\mathcal{B}^{*\prime}$) is determined to be governed by the CR $\mathbf{D}_{2d}(/\mathbf{C}_2')$.

Exercise 16. Discuss the stepwise procedure by using another assemblage pattern (**44**), where Fig. 15 is taken into consideration as a permutation diagram.

From the viewpoint of the intermolecular stereochemistry, the selection of the assembly $\mathcal{B}_1^{*\prime}$ ($\in \mathcal{B}^{*\prime}$) in the assembled mandala (**45**) corresponds to the selection of **1/4** (f_1/f_4), which pairs with its enantiomeric assembly, i.e., **6/9** (f_2/f_3). Thus, the orbit ($\mathcal{B}^{*\prime}$) is subdivided into two enantiomeric suborbits, i.e., $\{\mathcal{B}_1^{*\prime}, \mathcal{B}_3^{*\prime}\}$ and $\{\mathcal{B}_2^{*\prime}, \mathcal{B}_4^{*\prime}\}$ in agreement with the fact the CR $\mathbf{D}_{2d}(/\mathbf{C}_2')$ shows the enantiosphericity of the orbit ($\mathcal{B}^{*\prime}$).

From the viewpoint of the intramolecular stereochemistry, on the other hand, the selection of the assembly $\mathcal{B}_1^{*\prime}$ means that the vertices of the assembly (**1/4**) are divided into four orbits: $\{1,4\}$, $\{2,3\}$, $\{5,8\}$, and $\{6,7\}$. According to the division, an appropriate set of (pro)ligands or atoms ($\circ$ or $\bullet$) is placed on the vertices of the assembly (**1/4**) so as to generate molecules (**89–94**). The vertices of each of the molecules **89–94**) can be further segmented to give a segmented $\mathbf{C}_2'$-molecule (one of **95–100**). Replace each segment in the segmented $\mathbf{C}_2'$-molecule (**95–100**) by (pro)ligands (or atoms). Thereby, the corresponding $\mathbf{C}_2'$-molecule (one of **101–106**) is generated on the basis of an allene skeleton.

By the inspection of Figs. 21 and 22 and by the discussions described above, one can find the parallelism between the assemblage in a mandala and the segmentation in a regular body. Thereby, the intermolecular stereochemistry (stereoisomerism) and the intramolecular stereochemistry are discussed in a common framework, as summarized in Table 2.

4.2   Conventional Terminology

In the conventional stereochemistry for describing the intramolecular stereochemistry, the terms "enantiotopic", "diastereotopic", and "stereoheterotopic" have been used to specify the relationships between *two* sites (or ligands or other objects). On the other hand, the terms *enantiospheric*, *homospheric*, and *hemispheric* used in the USCI approach specify the nature of an orbit of *two or more* sites (or ligands or other objects), where the sphericity is the attribute of the orbit. The conventional term "enantiotopic" can be defined as having an extended meaning by means of the USCI approach, as shown in Table 3 [18]. The other conventional terms
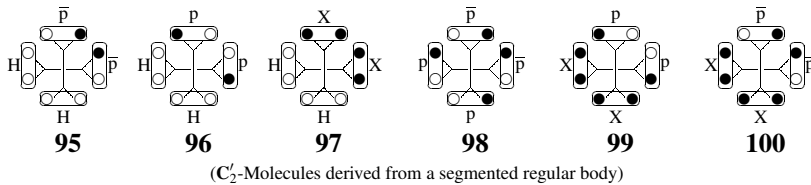
Intermolecular Stereochemistry (Stereoisomerism)
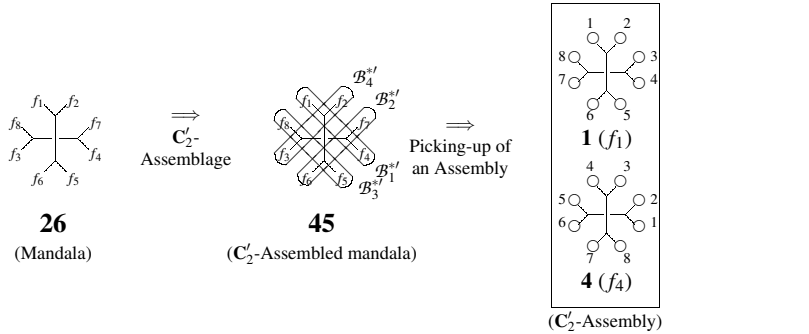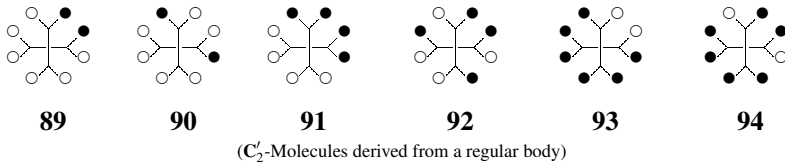
Intramolecular Stereochemistry
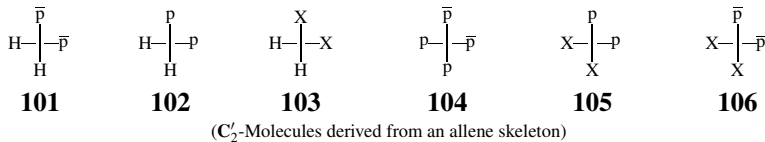
Figure 22: Mandala for $\mathbf{D}_{2d}$, an assembled mandala with a $\mathbf{D}_{2d}(/\mathbf{C}_2')$-orbit of $\mathbf{C}_2'$-assemblies, a $\mathbf{C}_2'$-assembly selected, $\mathbf{C}_2'$-molecules derived from a regular body, $\mathbf{C}_2'$-molecules derived from a segmented regular body and $\mathbf{C}_2'$-molecules derived from an allene skeleton.

Table 2: Terminology for the Parallelism between the Intramolecular Stereochemistry and the Intermolecular Stereochemistry

Intramolecular Stereochemistry	Intermolecular Stereochemistry
regular body (transformula)	mandala (nested regular body)
segment in a regular body	assembly in a mandala
orbit of segments	orbit of assemblies
(pro)ligand, atom	molecule

Table 3: Properties of an Orbit for the Intramolecular Stereochemistry [18]

orbit	properties
homospheric	A homospheric orbit can be present in an achiral molecule or an achiral regular body. Each member (ligand or other object or segment) of the orbit exhibits *achirotopic nature*, as shown by the symbol (◐).[a)] Each pair of members selected from the orbit is in *homotopic* (more descriptively, holotopic [20]) relationship. Each member should be achiral in isolation according to chirality fittingness [21, 10].
enantiospheric	An enantiospheric orbit can be present in an achiral molecule or an achiral regular body. The size of the orbit is even. The members (ligands or other objects or segments) of the orbit are divided into two halves by operating rotations (proper rotations) only. The one half contains ligands or other objects or segments (◖) as members, each of which exhibits *chirotopic nature*, while the other half contains ligands or other objects or segments of the opposite chirotopic nature (◗). The two halves are *enantiotopic* to each other, where any member of one half is enantiotopic to any member of the other half. Any two members in each half are *homotopic* (more descriptively, hemitopic [20]). Each member may be achiral or chiral in isolation according to chirality fittingness, where chiral ligands (or other objects or segments) exhibit a compensated chiral packing [21, 10]. A molecule having at least one enantiospheric orbit is *prochiral*.
hemispheric	A hemispheric orbit is present in a chiral molecule or a chiral regular body. Each member (ligand or other object or segment) of the orbit exhibits *chirotopic nature*, as shown by the symbol (◖). Each pair of members selected from the orbit is in *homotopic* (more descriptively, hemitopic [20]) relationship. Each member may be achiral or chiral in isolation according to chirality fittingness [21, 10].

[a)]For the symbols (◐, ◖, and ◗), see Part 1.

Table 4: Properties of an Orbit for the Intermolecular Stereochemistry

orbit	properties
homospheric	A homospheric orbit contains achiral transformulas (achiral molecules or achiral assemblies) on the basis of an achiral skeleton. Each member (transformula) of the orbit exhibits *achiral nature*. Each pair of members selected from the orbit is in *homomeric* relationship.
enantiospheric	An enantiospheric orbit contains chiral transformulas (chiral molecules or achiral assemblies) on the basis of an achiral skeleton. The size of the orbit is even. The members (transformulas) of the orbit are divided into two halves by operating rotations (proper rotations) only. The one half contains transformulas as members, each of which exhibits *chiral nature*, while the other half contains transformulas of the opposite chiral nature. The two halves are *enantiomeric* to each other, where any member of one half is enantiomeric to any member of the other half.
hemispheric	A hemispheric orbit contains chiral transformulas (chiral molecules or achiral assemblies) on the basis of a chiral skeleton. Each member (transformula) of the orbit exhibits *chiral nature*.

"diastereotopic" and "stereoheterotopic" can be defined as specifying the relationships between two orbits or more [19].

In the conventional stereochemistry for describing the intermolecular stereochemistry, the terms "enantiomeric", "diastereomeric", and "stereoisomeric" have been used to specify the relationships between *two* molecules. On the other hand, the term *enantiospheric* of the USCI approach specifies an orbit of equivalent molecules as an attribute of the orbit, which can derive the term "enantiomeric", as shown in Table 4. The term *homospheric* shows that each molecule of an orbit at issue is achiral. Thus, an enantiomeric pair of chiral molecules is contained in an enantiospheric orbit, while an achiral molecule is contained in a homospheric orbit. In other words, such an achiral molecule is regarded as a self-enantiomeric pair in the USCI approach.

The other conventional terms "diastereomeric", and "stereoisomeric" require more extended groups (*RS*-stereoisomeric groups and stereoisomeric groups) in order to be specified more strictly, as discussed elsewhere [22].

5 Mandalas, Assembled Mandalas, and Reduced Mandalas

Because the procedures of assemblage and of converting assemblies into molecules (Fig. 21 and 22) are somewhat artificial and mathematics-oriented, an alternative explanation is useful, where the procedures are reversely taken into consideration.

5.1 Spontaneous Assemblage

Consider that the eight transformulas contained in the mandala (**26**) of Fig. 21 are replaced by **18**–**25** (Fig. 7). This procedure generates another mandala shown in Fig. 23. When the numbering of the vertices is disregarded, **18** (f_1) and **22** (f_2) are regarded to be identical so that

they represents a $\mathbf{C}_s$-molecule. Each pair of **24** (f_7)/**20** (f_4), **19** (f_5)/**23** (f_6), and **25** (f_3)/**21** (f_8) represents a $\mathbf{C}_s$-molecule. The resulting $\mathbf{C}_s$-molecules are equivalent under $\mathbf{D}_{2d}$. As a result, the $\mathbf{C}_s$-assemblage is spontaneously accomplished. In other words, the four assemblies ($\mathcal{A}_1^*$, $\mathcal{A}_2^*$, $\mathcal{A}_3^*$, and $\mathcal{A}_4^*$) of **36** (cf. Fig. 21) are spontaneously replaced by the four assemblies ($\mathcal{A}_1^\dagger$, $\mathcal{A}_2^\dagger$, $\mathcal{A}_3^\dagger$, and $\mathcal{A}_4^\dagger$) of Fig. 7. It follows that Fig. 23 diagrammatically shows the CR $\mathbf{D}_{2d}(/\mathbf{C}_s)$ that governs an orbit containing the $\mathbf{C}_s$-molecule (**18**) via the orbit of the $\mathbf{C}_s$-assemblies ($\mathcal{A}_1^\dagger$, etc.).

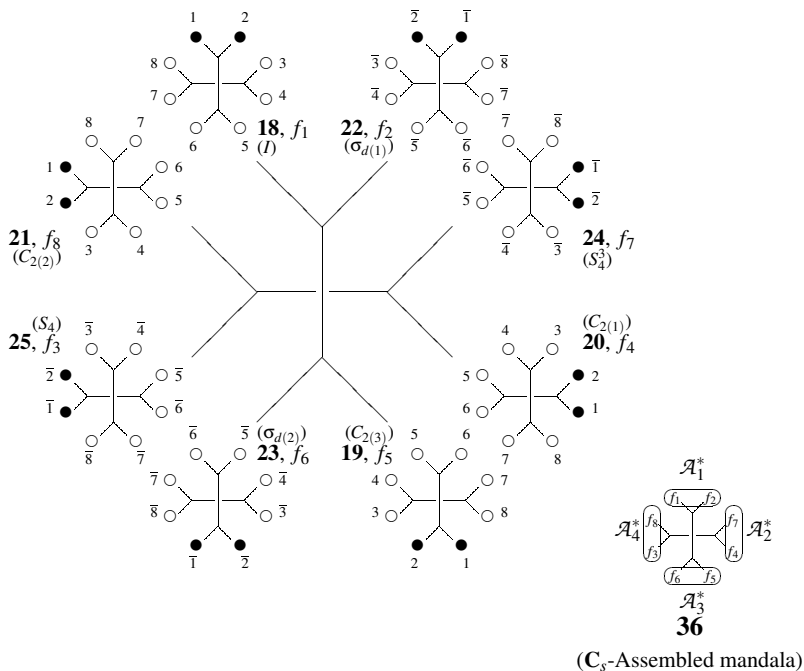($\mathbf{C}_s$-Assembled mandala)

Figure 23: Mandala that is equalized to a $\mathbf{C}_s$-assembled mandala (**36**), where a spontaneous $\mathbf{C}_s$-assemblage occurs. The two molecules of each pair (**18** (f_1)/**18** (f_2) **24** (f_7)/**20** (f_4), **19** (f_5)/**23** (f_6), or **25** (f_3)/**21** (f_8) are identical. The four pairs (assemblies) are equivalent under $\mathbf{D}_{2d}$ so that they construct an orbit governed by the CR $\mathbf{D}_{2d}(/\mathbf{C}_s)$.

Exercise 17. Following the procedure for constructing Fig. 23, show the corresponding diagrams for **72**–**76**.

Exercise 18. Following the procedure for constructing Fig. 23, show the corresponding diagrams for **89**–**94**.

The above discussions allow us to take the reverse direction of Fig. 21 or Fig. 22 (the step of "an assembly into a molecule"). Thus, the initial usage of Fig. 23 in place of the $\mathbf{C}_s$-assembled mandala (**36**) is rather convenient for the application of Fujita's USCI approach to chemical combinatorics. This subject will be discussed in Part 3 of this series.

5.2 Spontaneous Segmentation

Consider next that the eight transformulas contained in the mandala (**26**) of Fig. 21 are replaced by **83** and its permuted transformulas. This procedure generates another type of mandala, the vertices of which accommodate $\mathbf{C}_s$-molecules derived from an allene skeleton, as shown in Fig. 24. This type of mandalas is called *reduced mandalas*, where the $\mathbf{C}_s$-segmentation shown in the lower part of Fig. 21 are already taken into account. This feature is regarded as a spontaneous segmentation, which is mathematically equivalent to the spontaneous assemblage described in the preceding subsection. Moreover, a spontaneous $\mathbf{C}_s$-assemblage occurs so that **83** (f_1) and **107** (f_2) are regarded as being equivalent to generate a $\mathbf{C}_s$-molecule. Each pair of **108** (f_7)/**109** (f_4), **110** (f_5)/**111** (f_6), and **112** (f_3)/**113** (f_8) represents a $\mathbf{C}_s$-molecule. The resulting $\mathbf{C}_s$-molecules are equivalent under $\mathbf{D}_{2d}$. In other words, the four assemblies ($\mathcal{A}_1^*$, $\mathcal{A}_2^*$, $\mathcal{A}_3^*$, and $\mathcal{A}_4^*$) of **36** (cf. Fig. 21) are spontaneously replaced by the four equivalent molecules of the $\mathbf{C}_s$-molecule (**83**). Hence Fig. 24 diagrammatically shows the CR $\mathbf{D}_{2d}(/\mathbf{C}_s)$ that governs an orbit containing the $\mathbf{C}_s$-molecule (**83**) via the orbit of the $\mathbf{C}_s$-assemblies ($\mathcal{A}_1^*$, etc.).
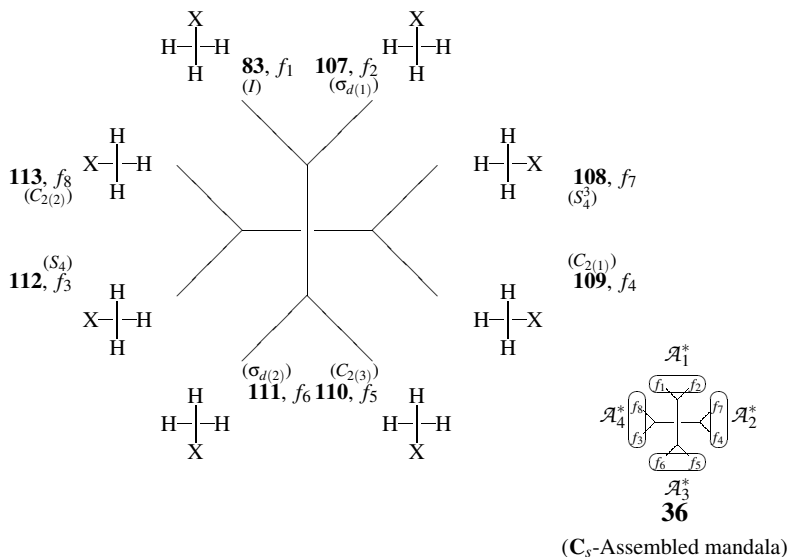

(**$\mathbf{C}_s$**-Assembled mandala)

Figure 24: Reduced mandala in which a spontaneous segmentation and a spontaneous $\mathbf{C}_s$-assemblage occur. Two molecules of each pair (**83** (f_1)/**107** (f_2), **108** (f_7)/**109** (f_4), **110** (f_5)/**111** (f_6), or **112** (f_3)/**113** (f_8)) are identical. The four pairs (assemblies) are equivalent under $\mathbf{D}_{2d}$ so that they construct an orbit governed by the CR $\mathbf{D}_{2d}(/\mathbf{C}_s)$. The reduced mandala exhibits the same symmetrical behavior as the $\mathbf{C}_s$-assembled mandala (**36**).

Exercise 19. Following the procedure for constructing Fig. 24, show the corresponding diagrams for **84–88**.

Exercise 20. Following the procedure for constructing Fig. 24, show the corresponding diagrams for **101–106**.

It should be noted that Fig. 23 can be considered as a special case of reduced mandalas, where a $\mathbf{C}_1$-segmentation (i.e., no segmentation) is considered in the step of segmentation.

The above discussions allow us to take the reverse direction of Fig. 21 or Fig. 22 (the steps of "an assembly into a molecule" "segmentation", and "segments into proligands"). Thus, the initial usage of the reduced mandala (Fig. 24) in place of the $\mathbf{C}_s$-assembled mandala (**36**) is straightforward for the application of Fujita's USCI approach to chemical combinatorics. This subject will be discussed in Part 3 of this series.

For the purpose of chemical combinatorics (Part 3), it is worthwhile to point out that an **H**-molecule (e.g., a $\mathbf{C}_s$-molecule **83**) which is derived from a **G**-skeleton with a $\mathbf{G}(/\mathbf{H}')$-orbit of substitution positions is characterized by the CR $\mathbf{G}(/\mathbf{H})$. The CR $\mathbf{G}(/\mathbf{H}')$ (e.g., $\mathbf{D}_{2d}(/\mathbf{C}_s)$ for Fig. 24) appears in an $\mathbf{H}'$-segmented regular body described in Part 1, so that the CR is characterized by each $\mathbf{G}(/\mathbf{H}')$-row of the subduction table, the USCI-CF table, the USCI table, and the mark table (e.g., Tables 8–11 of Part 1 for $\mathbf{G} = \mathbf{D}_{2d}$). On the other hand, the CR $\mathbf{G}(/\mathbf{H})$ (e.g., $\mathbf{D}_{2d}(/\mathbf{C}_s)$ for Fig. 24) appears in an **H**-assembled mandala (e.g., **36** in Fig. 24 for $\mathbf{H} = \mathbf{C}_s$) described in Part 2 (the present paper), so that the CR is characterized by each $\mathbf{G}(/\mathbf{H})$-row of the subdcution table, the USCI-CF table, the USCI table, and the mark table (cf. 3.3.2). It should be emphasized that the tables discussed diagrammatically for $\mathbf{G}(/\mathbf{H})$ in terms of assembled mandalas (cf. 3.3.2) and those discussed diagrammatically for $\mathbf{G}(/\mathbf{H}')$ in terms of segmented regular bodies (e.g., Tables 8–11 of Part 1 for $\mathbf{G} = \mathbf{D}_{2d}$) are both equivalent to the set of tables derived algebraically by coset decompositions of **G** by **H** or **H**′ (cf. Appendices of Fujita's book [10]). Thereby, the concept of sphericities based on the CRs works effectively in both intramolecular (Part 1) and intermolecular stereochemistry (Part 2). That is *a common theoretical framework*!

6   Conclusions

A regular body is defined as a skeleton of **G**-symmetry that has $|\mathbf{G}|$ vertices governed by the coset representation (CR) $\mathbf{G}(/\mathbf{C}_1)$. The regular body generates $|\mathbf{G}|$ transformulas on the action of **G**. The resulting transformulas are so equivalent as to construct an orbit governed by the CR $\mathbf{G}(/\mathbf{C}_1)$. An assembly of **H**-symmetry ($\mathbf{H} \subset \mathbf{G}$) is defined as a set of such transformulas as fixed by the action of **H**. The **H**-assembly causes the division of the transformulas to generate equivalent **H**-assemblies, where the resulting set of **H**-assemblies constructs an orbit of **H**-assemblies. The orbit of **H**-assemblies is governed by the CR $\mathbf{G}(/\mathbf{H})$. Each **H**-assembly corresponds to an **H**-molecule derived from a skeleton of **G**-symmetry. Thus the CR $\mathbf{G}(/\mathbf{H})$ is concluded to control the intermolecular stereochemistry (stereoisomerism), where it provides us with alternative method of obtaining subduction tables, USCI-CF tables (tables of unit-subduced-cycle-index with chirality fittingness), USCI tables (tables of unit-subduced-cycle-index without chirality fittingness), and mark tables, which have been described in Part 1.

A mandala is defined as a hypothetical structure (a nested regular body) in which the $|\mathbf{G}|$ transformulas generated as above from a regular body by the action of **G** are placed on the vertices of a regular body. By using the mandala, the selection of the **H**-assemblies described above is demonstrated diagrammatically. Intermolecular and intramolecular stereochemistries are integrated by defining assembled mandalas and reduced mandalas.

References

[1] Fujita, S. (2005) *MATCH Commun. Math. Comput. Chem.* **54**, 251–300.

[2] Hinze, J. eds. (1979) *The Permutation Group in Physics and Chemistry (Lecture Notes in Chemistry 12)* (Springer-Verlag, Berlin Heidelberg).

[3] Brocas, J., Gielen, M., & Willem, R. (1983) *The Permutational Approach to Dynamic Stereochemistry* (McGraw-Hill International, New York).

[4] Ugi, I., Dugundji, J., Kopp, R., & Marquarding, D. (1984) *Perspectives in Theoretical Stereochemistry* (Springer-Verlag, Berlin-Heidelberg).

[5] Pólya, G. (1937) *Acta Math.* **68**, 145–254.

[6] Pólya, G. & Read, R. C. (1987) *Combinatorial Enumeration of Groups, Graphs, and Chemical Compounds* (Springer-Verlag, New York).

[7] Balaban, A. T. eds. (1976) *Chemical Applications of Graph Theory* (Academic Press, London).

[8] Fujita, S. (2005) *Theor. Chem. Acc.* **113**, 73–79,
Online: http://www.springerlink.com/index/10.1007/s00214-004-0605-0.

[9] Fujita, S. (2005) *Theor. Chem. Acc.* **113**, 80–86,
Online: http://www.springerlink.com/index/10.1007/s00214-004-0606-z.

[10] Fujita, S. (1991) *Symmetry and Combinatorial Enumeration in Chemistry* (Springer-Verlag, Berlin-Heidelberg).

[11] Fujita, S. (1990) *J. Math. Chem.* **5**, 99–120.

[12] Fujita, S. (2001) *J. Math. Chem.* **30**, 249–270.

[13] Fujita, S. & El-Basil, S. (2002) *MATCH Commun. Math. Comput. Chem.* **46**, 121–135.

[14] Fujita, S. & El-Basil, S. (2003) *J. Math. Chem.* **33**, 255–277.

[15] Fujita, S. & El-Basil, S. (2004) *J. Math. Chem.* **36**, 211–229.

[16] Fujita, S. (2001) *Bull. Chem. Soc. Jpn.* **74**, 1585–1603.

[17] Fujita, S. (2002) *Bull. Chem. Soc. Jpn.* **75**, 1949–1962.

[18] Fujita, S. (2004) *J. Comput. Chem. Jpn.* **3**, 113–120.

[19] Fujita, S. (1990) *Tetrahedron* **46**, 5943–5954.

[20] Fujita, S. (2000) *Bull. Chem. Soc. Jpn.* **73**, 1979–1986.

[21] Fujita, S. (1990) *J. Am. Chem. Soc.* **112**, 3390–3397.

[22] Fujita, S. (2004) *J. Org. Chem.* **69**, 3158–3165.